

April 2014

Design of a Three Dimensional Scaffold to Grow Cartilaginous Thick Tissue

Andrew Christian Leverone
Worcester Polytechnic Institute

Jeremy Harris Kibby
Worcester Polytechnic Institute

Samuel Casey Eisenberg
Worcester Polytechnic Institute

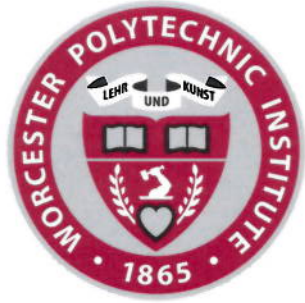
Tara Brittany Meinck
Worcester Polytechnic Institute

Follow this and additional works at: <https://digitalcommons.wpi.edu/mqp-all>

Repository Citation

Leverone, A. C., Kibby, J. H., Eisenberg, S. C., & Meinck, T. B. (2014). *Design of a Three Dimensional Scaffold to Grow Cartilaginous Thick Tissue*. Retrieved from <https://digitalcommons.wpi.edu/mqp-all/534>

This Unrestricted is brought to you for free and open access by the Major Qualifying Projects at Digital WPI. It has been accepted for inclusion in Major Qualifying Projects (All Years) by an authorized administrator of Digital WPI. For more information, please contact digitalwpi@wpi.edu.



WPI

Design of a Three Dimensional Scaffold to Grow Cartilaginous Thick Tissue

A Major Qualifying Project Report

Submitted to the Faculty of

WORCESTER POLYTECHNIC INSTITUTE

In partial fulfillment of the requirements for the

Degree of Bachelor of Science

Authored By

Samuel Eisenberg

Jeremy Kibby

Andrew Leverone

Tara Meinck

Four handwritten signatures in black ink are written over horizontal lines. From top to bottom, they correspond to Samuel Eisenberg, Jeremy Kibby, Andrew Leverone, and Tara Meinck.

Date Approved: May 1st, 2014

Approved by:

Professor Domhnall Granquist-Fraser, Ph.D.

Professor Sakthikumar Ambady, Ph.D.

Professor Gregory Fischer, Ph.D.

Abstract

Damage to avascular tissue often requires medical attention due to its inability to regenerate healthy tissue. Tissue engineering has the potential to repair this damage by growing thick tissue *in vitro* with properties and geometry similar to the innate tissue by seeding three dimensional (3D) scaffolds in hydrogels. Scaffold designs must increase internal surface area and void fraction to provide nutrients to the center of the scaffold to ensure viability and sustainable growth.

Authorship

All team members contributed equally to the creation of this report.

Acknowledgements

The authors of this paper would like to thank the following individuals:

- Professors Ambady, Granquist-Fraser, and Fischer for advising and supporting our team
- The previous team members of the DGF111A and DGF111B MQP groups that worked on this research and laid the foundation for this project
- Cathy McEleney and Dariusz Pryputniewicz from Draper Laboratories who allowed us to use their facilities to print more scaffolds using their 3D printer
- David Ciolfi from Technology Education Concepts, Inc. and Doctor Robert Meislin for their assistance with obtaining a 3D printer
- Hans Snyder and Lisa Wall for their assistance in the laboratory
- Nick Trabucco and Professor Planchard for the use of their 3D printers.

Table of Contents

1 – Introduction	9
2 – Literature Review	9
2.1 – 3D Printing.....	10
2.1.1 – Printer History	10
2.1.2 – Organ Printing/Bioprinting.....	11
2.1.3 – 3D Scaffold Printing.....	12
2.2 – Cartilage/Tissue Engineering.....	13
2.2.1 – Bioreactors	13
2.2.2 – Thick Tissue Culture	14
2.3 – Case Study: The Meniscus.....	14
2.3.1 - Relevance.....	14
2.3.2 – Meniscal Tears and Treatment	15
2.3.3 – Biomechanics of Meniscus.....	16
2.3.4 – Porous Scaffolds.....	17
2.4 – Histology Analysis.....	18
2.4.1 – Viability Assays	18
2.4.2 – Destructive Analysis	19
2.4.3 – Non-Destructive	20
2.5 – Cell Culture.....	20
2.5.1 – Overview	20
2.5.2 – Primary Chondrocytes.....	21
2.5.3 – Mesenchymal Stem Cells	21
2.5.4 – Cancer-Derived Cells	22
2.5.5 – Growth Factors for Chondrogenesis	23
3 – Project Strategy.....	23
3.1 – Original Client Statement.....	23
3.2 – Objectives.....	24
3.2.1 – Objectives Overview	24
3.2.2 – Quantifiable Objective Comparison	25
3.3 – Constraints	26
3.4. Revised Client Statement.....	26
3.5 – Project Approach.....	27

3.6 Biocompatible material.....	27
4. Methods and Design Alternatives.....	28
4.1 3D printer modification.....	28
4.1.1 MakerBot® Extruder Nozzles	28
4.1.2 MakerBot® Replicator Problems.....	29
4.1.3 MakerBot® Software.....	31
4.2 Scaffold Design.....	33
4.2.1 Fractal Generation	34
4.2.2 Gross Scaffold Structure	34
4.3 Alternative Scaffold Designs	36
4.4 PLA Degradation Methodology.....	37
4.5 ATDC5 Differentiation Protocol	37
4.5.1 BrdU Assay	39
4.5.2 Alcian Blue Staining.....	39
4.5.3 Modified Serum Levels.....	39
4.6 Hydrogel Protocol	40
4.6.1 Cellular Distribution Methodology	41
4.6.2 ATDC5 Differentiation in Collagen Hydrogel.....	41
4.7 Scaffold Seeding Methodology	41
4.8 Tissue Culture Protocol.....	43
4.9 Modular Scaffold Protocol	44
4.10 Histology Methodology and Testing	44
4.10.1 Scaffold Toughness	45
4.10.2 Scaffold Adherence to Scaffold.....	45
4.10.3 Scaffold Staining.....	47
5. Design Verification.....	47
5.1 Cell Feasibility	47
5.1.1 BrdU Results.....	47
5.1.2 Alcian Blue Staining.....	49
5.1.3 Modified Serum Level Results.....	51
5.1.4 Cellular Distribution Results.....	53
5.1.5 ATDC5 Differentiation in Collagen Hydrogel Results	54
5.2 PLA Degradation Results.....	56

5.3 Histology Results	57
5.4 Modular Scaffold Results	59
6. Discussion.....	60
6.2 Economics	61
6.3 Environmental impact.....	62
6.4 Societal influence	62
6.5 Political ramifications.....	63
6.6 Ethical concerns	63
6.7 Health and safety issues	63
6.8 Manufacturability	63
6.9 Sustainability.....	64
7 Final Design	64
8 - Conclusions and Recommendations.....	67
8.1 - Objectives	67
8.2 - Future Improvements	67
8.3 - Clinical Importance	69
References	70
Appendices:.....	74
Appendix A: Cell Passaging	74
Appendix B: Alcian blue staining protocol	74
Appendix C: Scaffold seeding protocol	74
Appendix D: Modular Scaffold Separation.....	75
Appendix E: Histological Tissue Processing and Microtome Sectioning.....	76
Appendix F: Hematoxylin and Eosin Staining Protocol	76
Solutions:	77
Appendix G: Cell Folding Images.....	78

Table of Figures

Figure 1: Diagram of Meniscus and Common Tears (Healthware Inc., 2012)	15
Figure 2: Meniscal Displacement is Represented by the Dotted Lines (mm) (Fox, A. <i>et al.</i> , 2011).....	17
Figure 3: Objectives Tree	24
Figure 4: Simple "Sphere-in-Cube" Generated in OpenSCAD.....	35
Figure 5: Errors in SolidWorks Surface Mesh Converted. Left - Guided Process; Right - Automatic Process	35
Figure 6: Different Menger Sponge Fractals. Left - 3rd Level menger Sponge; Right - 2nd Level menger Sponge	37
Figure 7: Sterilization During Seeding Process.....	42
Figure 8: Seeded Scaffolds in Wells	43
Figure 9: Seeded Scaffolds Covered in Media.....	44
Figure 10: Photo of Scaffolds Dissociated from Slides in Water.....	46
Figure 11: Results of Glue Tests on Empty Scaffolds. Left-Right: H&E Stain with Loctite, H&E Stain with Liquid Nails, NFR Stain with Liquid Nails, NFR Stain with Loctite	47
Figure 12: Results of BrdU assay with 25µm Scale Bars	49
Figure 13: Results of Ascorbic Acid Enhanced Differentiation Procedure.....	51
Figure 14: Results of modified serum level on ATDC5 differentiation	53
Figure 15: Results of cellular distribution experiment with 25µm scale bars	54
Figure 16: Results of ATDC5 Differentiation within Collagen hydrogel.....	56
Figure 17: H&E Staining of 5µm Scaffold Slices at Different Depths	58
Figure 18: Phalloidin/DAPI Staining of Scaffolds. Left-Right: Phalloidin Stain, DAPI Stain, Phase Contrast Image	59
Figure 19: Sectioned and Stained Modular Scaffold Compared to a Negative Control	60
Figure 20: CAD Model of Modular Scaffold Sections of 2nd Level Recursion Cylindrical Menger Sponge - Cross Sectioned View.....	64
Figure 21: 3D Printed PLA Modular Scaffold Sections of Second Level Recursion Cylindrical Menger Sponge (Left to Right: Top Down View, Stacked Side View).....	65

Table of Tables

Table 1: Percentages of Sports Related Ijuries with Respect to Age (LaBella, M., 2007)	15
Table 2: Range of Tibiofemoral Joint Motion in the Sagittal Plane During Common Activities (Nordin, M. <i>et al.</i> 2001)	16
Table 3: Pairwise Comparison Chart	25
Table 4: Ascorbic Acid Enhanced ATDC5 Media	38
Table 5: ATDC5 Differentiation Media	38
Table 6: ATDC5 Differentiation Media with Reduced FBS and 2% AHS.....	39
Table 7: ATDC5 Differentiation Media with 2% AHS.....	40
Table 8: Degradation Results	56

1 – Introduction

Avascular cartilage, such as that found within the knee meniscus, does not have the regenerative capabilities of other tissues. This is largely due to low nutrient flow caused by the lack of blood vessels running throughout the tissue. Currently, any tears or wounds that occur in avascular cartilage cannot be healed and must be treated by either removing damaged sections of the tissue or complete removal of the cartilage, as in a meniscectomy. Alternative treatment for avascular cartilage tears, such as tissue engineering, could provide a solution to this problem. However, tissue engineering thick, avascular tissue *ex vivo* leads to some of the same issues as *in vivo* healing. A current challenge with growing thick tissue is mitigating with the necrosis of cells within the center of the tissue when it is grown using three dimensional culture. Cell necrosis occurs from a lack of proper nutrient penetration within the tissue culture and is usually seen within tissue culture greater than 1mm. This project aimed to improve the clinical treatment for improved avascular cartilage treatment via the creation of a 3-dimensional (3D) biodegradable scaffold that could prevent cell necrosis in thick tissue culture.

The scaffold was modeled in CAD software and then printed using a desktop 3D printer. The scaffold was designed to fulfill the cells proliferatory needs in order for the tissue to successfully grow. The material Poly-Lactic Acid (PLA) was used as it is compatible with 3D printing, biocompatible, and biodegradable, which were essential material properties for this project.

Cells from the ATDC5 mouse cell line were cultured to produce chondrocytes, which were then seeded onto the printed scaffold using a collagen hydrogel. Cell proliferation was scaled to coincide with degradation of the scaffold so that the chondrocytes form avascular cartilage as the scaffold degrades. Once cultured in the lab, the viability of the tissue engineered cartilage will be validated through histological testing.

2 – Literature Review

This report describes the methodology and results of growing cartilaginous thick tissue using a 3D printed biodegradable scaffold. Pertinent research regarding 3D printing, tissue engineering, and methods of histological analysis are summarized in the following literary review.

2.1 – 3D Printing

2.1.1 – Printer History

A growing frontier in the field of modern tissue engineering has been the increasing usage of three dimensional (3D) printers for organ printing and scaffold creation for tissue growth. These printers allow for the construction of live tissue in what can be considered a relatively short period of time when compared to other methods used for tissue growth. These 3D printed tissues can be custom made for each patient and made from the patients' own cells. Once printed the tissue or organs can then be placed inside the patient to repair or replace damaged tissue (Melchels 2005).

The inception of 3D printing can be traced back to the late 1940's, right after World War II, when John Parsons invented numerical control for manufacturing machines. What this means is that any machine used in the manufacturing process has every parameter and variable controlled by a computer, where before these processes had to be done by hand (Bradshaw *et al.* 2010). This idea of allowing a computer to automate the manufacturing process was a turning point in the manufacturing industry as it allowed a process once done by humans to be completely automated. It wasn't until the 1970's though that the combination of a joke and numerical controls would lead to the birth of the 3D printing industry. In 1974 David Jones would write a small joke in his column in *New Scientist* that lasers could be shone into a liquid plastic monomer and cause the monomer to solidify. Jones expounded upon his joke by proposing that the wavelengths could be adjusted so that solidification of the polymer could only be achieved when two separate beams intersected (Bradshaw *et al.* 2010). This entire process would be computer controlled to ensure proper deflection of the lasers.

What initially started off as a tongue-in-cheek joke was soon made reality when Wyn Kelly Swainson was granted a patent for a similar idea in 1977. Swainson's patent used a laser to cause covalent crosslinking of a liquid monomer at its surface while the object being created rested on a tray that was lowered as more material was added to the object. This was the start of the 3D printing industry and the industry rapidly grew in the following years. One reason for 3D printing's rapid growth was thanks to the lack of need to use tool path calculations to cut away material. Since material is being added, layer by layer, to a constant flat surface by a laser it is much easier to write a program to control the process of manufacturing (Bradshaw *et al.* 2010).

While 3D printing is slightly less accurate than forming an object by removing material it allows for the creation of complex and intricate shapes.

2.1.2 – Organ Printing/Bioprinting

One area of research in 3D printing includes the direct printing of tissue and organs through the use of cell seeded hydrogels. This process is called organ printing or bioprinting and is the process by which tissue and organs are created through the deposition of cells, layer by layer, in a hydrogel onto a sterile surface. This process is aided by computer aided design (CAD) software to accurately layer the hydrogel into the proper form where a model is created using CAD and that model is then uploaded to the 3D printer. The printer will then read the model file and begin to create the tissue/organ model layer by layer (Mirinov 2003). Cells within the hydrogel will begin to mature and vascularize into living tissue. Different types of tissue and organ printing include jet-based cell printers, biplotters, and cell dispensers.

Currently organ printing is a three step process of pre-processing, processing, and post-processing of organs (Mirinov 2003). In pre-processing a CAD model of the tissue to be printed is created and this model acts like a blueprint of the tissue. It must accurately replicate the model to ensure that the printed tissue replicated the biomechanical properties of the in-vivo tissue. In the processing phase the CAD model is used to actually print the tissue using a 3D printer. This is usually done through the process of layering hydrogels into the 3D model. Finally, post-processing is the process in which the cell seeded hydrogel is cultivated until the cells have differentiated into the proper tissue.

Some advantages that current 3D bioprinting methods have when compared to other printing methods include precise spatial placement of cells during printing, precise placement of various biomaterials, and multiple placement of cell types such as smooth muscle and endothelial cells (Ozbolat *et al.* 2013). This method of 3D printing can also be classified into 3 categories which are as follow; laser based printing, inkjet based printing, and extrusion based printing.

2.1.2.1 – Laser Printing

Laser printing is the process by which trypsinized and centrifuged cells are suspended in a hydrogel with an adequately determined viscosity (Chichkov *et al.* 2013). This hydrogel is then placed between two glass slides with the upper slide called the donor slide and bottom slide called the collector slide. The donor slide is covered with a radiation absorbing layer material to

absorb the laser and a thin layer of material containing the cells and then placed a few hundred micrometers above the collector slide. A laser pulse is then sent through the slides which is absorbed by the donor slide and creates a shockwave that propels the cells onto the collector slide (Ozvolat 2013). This process is repeated to create the 3D object.

2.1.2.2 – Inkjet Printing

Inkjet printing is a 3D printing technique in which living cells are formed into droplets within the printer which then takes a digital image of what is to be printed and reproduced the digital image on a substrate with the cell ink droplets (Boland *et al.*, 2006). This method of printing allows for very small scale printing of items such as complex integrated circuits and biosensors. Inkjet printers can also be modified to allow for additional print heads that can deposit multiple cell types, which would allow for heterocellular tissue (Ozbolat *et al.* 2013). Inkjet cartridge design has also shown to allow for precise spatial delivery of multiple cell types in situ (Binder 2011).

2.1.2.3 – Extrusion-Based Deposition

Extrusion-based printing is the process by which cylindrical struts, composed of certain biomaterials and a cell solution, are continuously extruded onto a base. This base is coated with chemical crosslinkers that cause the cells to begin crosslinking in the biomaterial upon extrusion upon the base (Ozbolat *et al.* 2013). Extrusion-based printing shows potential for direct organ printing thanks to its cell patterning capability.

2.1.3 – 3D Scaffold Printing

A second method of 3D printing for tissue and organs is the creation of biodegradable scaffolds onto which cells are seeded and allowed to grow into the tissue and organs. Similar to organ printing the first step in scaffold creation is through the modeling of living tissue with the use of CAD. A 3D model of the tissue or organ is created to accurately replicate either the complete tissue or the section of damaged tissue that must be repaired. Once the model is completed a porous scaffold can be generated that will be printed layer by layer using a 3D printer. This scaffold must meet many requirements such as proper replication of biomechanical properties, proper nutrient delivery to the seeded cells, an optimal degradation rate of the scaffold material (Pfister 2003) and optimal ratio of scaffold material to pores. If the scaffold cannot properly replicate the biomechanical properties of the tissue than the cells may not accurately differentiate into the tissue with the proper biomechanical properties and the scaffold

itself could collapse and destroy the cells. Nutrient delivery is also important to ensure the viability of the tissue being grown for implant, the scaffold must ensure that the cells within the center do not die. Finally if the scaffold cannot degrade at a rate matching the growth and proliferation of the cells then the cells will cease proliferation and begin differentiation.

2.2 – Cartilage/Tissue Engineering

2.2.1 – Bioreactors

Bioreactors are devices engineered to promote biological growth and activity. There are many advantages of using a bioreactor to culture tissue as opposed to traditional static methods. These systems replicate physiological conditions and allow for the delivery of mechanical stimuli. Alterations made to these parameters can result in cellular differentiation and changes to the extracellular matrix (ECM) they secrete. Controlling pH, media flow, and mechanical stimuli that tissue engineered cartilage experience in vivo can be used to produce a tissue with a homogenous distribution of viable cells along with ECM that provides similar mechanical properties to natural cartilage (Athaniou 2003). For instance metabolism of ECM components is most efficient in chondrocytes cultured in pH ranging from 6.9 to 7.2 (Pazzano 1999).

Flow of culture media is also a common function for bioreactors used in tissue engineering applications. Exposing tissue engineered (TE) cartilage to fluid movement with a velocity of 1 $\mu\text{m/s}$, similar to movement of fluid within joints, while culturing tissue results in more ECM being secreted by the cells along with perfusivity of the media throughout scaffolds. Media flow and perfusion throughout a seeded scaffold is important when a homogenous distribution of living cells and matrix is desired. Increased mass transfer of nutrients and waste products between the media and cells throughout the tissue engineered construct will result tissue that is similar to natural tissue when compared histologically (Pazzano 1999).

Collagen types I and II as well as glycosaminoglycan (GAG) are components of the ECM of the meniscus, and the distribution, concentration, and orientation of them gives the meniscus its unique mechanical properties. Bioreactors that include a computer controlled piston can produce hydrostatic pressure that is evenly distributed upon cells seeded in a scaffold. Chondrocytes experience forces of 7 – 10 MPa in joints during normal day to day activities. Tailoring the magnitude of mechanical stimuli to the cells to what they would experience in the body leads to a tissue engineered product more congruent with the cartilage it would potentially

replace in the body, making this a promising technique when culturing tissue to be used as a transplant. Tissue engineered cartilage grown within bioreactors capable of cyclical mechanical stimuli within this physiological range have been shown to increase final amounts of collagen types I and II and GAG as well as mRNA used to produce them. Quantitative PCR used on samples of tissue engineered cartilage cultured within this type of bioreactor displayed a 9 fold increase in collagen coding mRNA and a 21 fold increase in GAG containing proteoglycan coding mRNA. (Athaniou 2003).

2.2.2 – Thick Tissue Culture

The generation of thick tissue structures is a challenge faced in the field of tissue engineering. Cells towards the surface of the scaffold are well supplied with nutrients from the media and the waste they produce is removed efficiently, but necrosis is often observed in the center where diffusion limits this mass transfer. One attempt to remedy this problem is through the incorporation of vascularization systems to scaffold design. Just as the body's vascular system overcomes the limits posed by diffusion through tissues, channels and systems of capillaries can be designed to mimic this and increase mass transfer in thick tissue culture (Ko *et al.* 2007).

2.3 – Case Study: The Meniscus

2.3.1 - Relevance

The meniscus is one example of a thick, avascular, cartilaginous tissue that would benefit from this kind of tissue engineering method. The lateral and medial menisci are the cartilaginous crescent-shaped wedges which provide lubricant and shock absorption to the knee joint. The knee menisci are often torn in sports-related injuries and degenerate in people aged 65 and older. Meniscal avascularity in fully developed tissue makes it difficult for the meniscus to heal when injured. The meniscus' composition changes as the body matures. A fetal meniscus is highly vascularized to promote growth but this vascularization decreases as the body matures and the knee joint bears weight (i.e. from crawling and walking.) The meniscus is left with 20% vascularization, most of which lies in the periphery of the cartilage, as seen in the image below in the “Red Zone” of the cartilage, while the remaining “White Zones” of the meniscus are avascular. Damage to the avascular “White Zone” of the menisci often require surgical reparations since the tissue cannot regenerate. The frequency and treatment of meniscal tears are discussed in the following section.

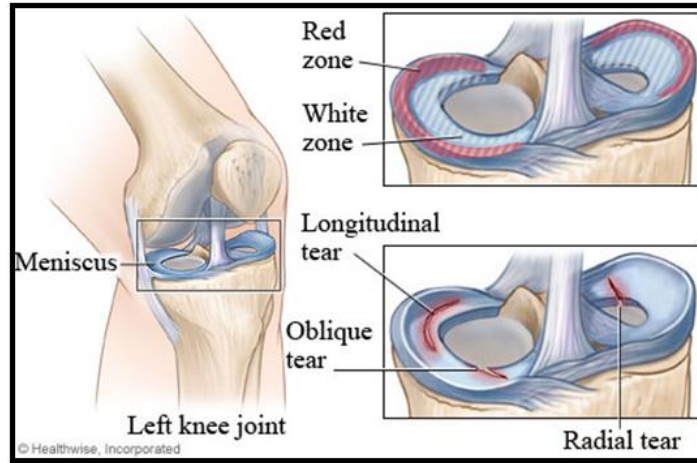


FIGURE 1: DIAGRAM OF MENISCUS AND COMMON TEARS (HEALTHWARE INC., 2012)

2.3.2 – Meniscal Tears and Treatment

Meniscal tears are the most common knee injuries and often coincide with other knee injuries, such as ACL tears. Once the knee joint has been afflicted with an injury, it is more likely to be reinjured. There are many mechanisms of injury that can cause the meniscus to tear, including acute twisting and impact at the knee joint, getting up from a squatting position and loading the knee from a fixed position (LaBella, M., 2007.) In individuals under 20 years old, every 11 of 12 meniscal tears are sports induced. As the focus group gets older, less meniscal injuries are attributed to sports injuries and more degenerative tears are present.

TABLE 1: PERCENTAGES OF SPORTS RELATED IJURIES WITH RESPECT TO AGE (LABELLA, M., 2007)

Age Range	% of Sports Related Injuries
<20	91.7
20-29	64.5
30-39	30.6
40-49	19.6
50-59	14.3

While not all meniscal tears are symptomatic, common symptoms are swelling, pain in the joint, pain when squatting or kneeling, locking, and loss of extension of the knee joint.

Depending on the severity of the symptoms and MRI of a meniscal tear depend on the route to recovery one takes. Menisci that must be treated undergo rehabilitation via physical therapy and/or surgery including either the repair or removal of the cartilage. Surgery is generally chosen as the recovery method when the tear; is in the avascular zone, therefore lacking the ability to heal itself properly, is longer than 5-8 millimeters in length, or is so painful daily function is limited. Annually, there are approximately 500,000 - 1,000,000 meniscal operations performed in the United States, grossing to \$4 billion. Physical therapy is needed after surgery as well as when it is the primary recovery mechanism. A patient generally undergoes two phases of physical therapy, the first where the therapist tries to reduce swelling and the second where the therapist focuses on strengthening and stabilizing the joint. A meniscal injury that requires medical attention is both slow to heal and expensive to treat.

2.3.3 – Biomechanics of Meniscus

The biomechanics of the menisci is essential to the knees functionality as discussed earlier. The menisci are kinematic bodies; they move as forces are exerted on them from the knee joint. The flexion and extension of the knee joint ranges for the different activities humans do, as shown in the table below.

TABLE 2: RANGE OF TIBIOFEMORAL JOINT MOTION IN THE SAGITTAL PLANE DURING COMMON ACTIVITIES (NORDIN, M. ET AL. 2001)

Activities	Range of motion from Knee extension to Flexion (Degrees)
Walking	0-67
Climbing Stairs	0-83
Descending Stairs	0-90
Sitting Down	0-93
Tying a Shoe	0-106
Lifting an Object	0-117

The lateral meniscus moves 3-5 times more than the medial meniscus in flexion (Brantigan, 1941) (DePalma, 1957.) Figure 2 shows the mean movement, of the menisci in millimeters. Areas where the meniscal movement is inhibited and there is little displacement, such as the posterior horn of the medial meniscus, are especially prone to impact injury because they are not compliant like the rest of the tissue (Fox, A. *et al.*, 2011) The stresses exerted on the meniscus are largely compressive due to the load exerted by the body's weight. The stresses on the meniscus are circumferential "hoop" stresses, which are then converted to axial forces and tensile stresses along the circumferential collagen fibers of the meniscus (Fox, A. *et al.*, 2011) The meniscus also absorbs shock; a knee joint with a meniscus absorbs 20% more shock than a knee joint with a meniscectomy (Fox, A. *et al.*, 2011) The menisci play an important role in stabilizing the knee joint; they are compressed by rounded femoral condyles, splaying out to create a flatter, more stable surface. The micro-canals of the meniscus, which are located near the periphery of the cartilage, act to transport nutrients to the joint through the synovial fluid.

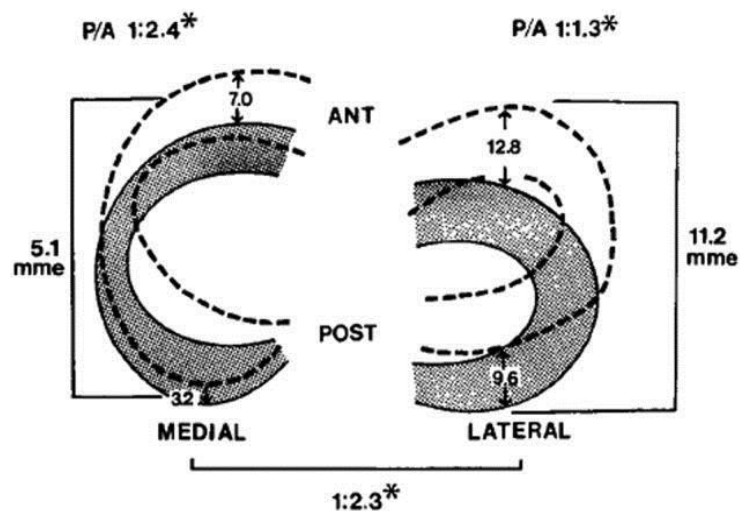


FIGURE 2: MENISCAL DISPLACEMENT IS REPRESENTED BY THE DOTTED LINES (MM) (FOX, A. *ET AL.*, 2011)

2.3.4 – Porous Scaffolds

Many biological tissues are porous, which can be measured by the ratio of void space to the total volume of the sample. The porosity of biological tissues allows the transfer of blood, oxygen, and other nutrients. The tortuosity is the measurement of resistance fluid meets when

traveling through the pores. Galban, et. al. explored the proliferation of chondrocytes generated on a porous, polymer scaffold to be used for repairing joint damage. Porous scaffolds were explored so the scaffold could mimic biotransport of nutrients via diffusion, as the tissue would undergo *in vitro* so the cells can live (Galban et.al., 1999.) The degradation of the polymer was much assumed much slower than the proliferation of the cells and, therefore could be ignored. Other studies, such as that done by Hollister, S., utilize a biodegradable polymer in which the rate of degradation must be compared to the cell growth rate (Hollister, 2006.) When degradable polymers are used in scaffolds, the effects on the scaffold's structural integrity must be taken into account with respect to the weight of the cells as they proliferate. The microstructures given by the porosity will give different effective stiffness and internal stresses. The porosity of the scaffold allows the necessary biological reactions to occur, as described above.

2.4 – Histology Analysis

2.4.1 – Viability Assays

Cellular viability can be quantified through the use of various assays. Life Technologies makes a two part viability kit that distinguishes between live and dead cells. Live cells with intact membranes and esterase activity are tagged with calcein-AM and fluoresce green while dead cells are stained with ethidium homodimer-1 which fluoresces red. This makes for easy distinction between living and dead cells and results in great images using fluorescent microscopy. However the proper ratio of the two ingredients needs to be determined before using this technique because this changes from tissue to tissue (Life Technologies 2005).

There is also a cytotoxicity colorimetric assay available from Abcam. The protocol calls for the assay solution to be incubated with cells as well as creating controls to compare to the cells. The assay is performed with microplates and a microplate reader sensitive at 570nm as well as 605nm. The ratio of absorbance at each wavelength is compared with the data from the controls and is used to determine percent cell viability (Abcam 2012).

Lastly, there is a class of cell viability assays that involve transfecting the cells with a DNA sequence. A canonical method is the Luciferase assay, which uses the DNA of the bioluminescent enzyme from either fireflies (*Metridia luciferase*) or sea pansies (*Renilla luciferase*) (Konopka, 2010; Shifera, 2010). A DNA plasmid with the sequence can be expanded

in *E. coli*, and then added to the cell culture via transfection (Coombe, 1998; Konopka, 2010; Shifera, 2010). The enzyme emits a specific frequency of light immediately after being transcribed (509nm for *Renilla* and 690nm for *Metridia*) and quickly breaks down upon cell death (Coombe, 1998; Shifera, 2010). These two characteristics make luciferase ideal for use in cell viability or cell growth assays.

2.4.2 – Destructive Analysis

Immunohistochemistry is a novel strategy for the histological analysis of tissue engineered or natural cartilage. Antibodies can target components of the ECM that are important to the overall mechanical properties and type of cartilage. For instance, the fibrocartilage that composes the medial meniscus contains collagen types I and II, GAG, and aggrecan within the extracellular matrix. Antibodies can then be used to hybridize specifically to any one of these (Verdonk *et al.* 2005). Allowing florescent microscopy to be used to analyze tissue engineered cartilage and quantitatively compare it to images of natural cartilage (Zhang *et al.* 2004).

Reverse transcription polymerase chain reaction (RT-PCR) can be used to measure RNA coding for constituents of the ECM produced by chondrocytes in tissue engineered cartilage. Levels of RNA can be compared between tissue engineered and natural menisci or even levels of RNA in different regions of the same tissue can be compared. In this process RNA is isolated, reverse transcribed into its complementary DNA (cDNA), and marked with a fluorescent tag so it can be quantitatively measure as it is being amplified in a fluorescently sensitive thermal cycler. Using this technique to measure gene expression in a tissue is a novel method for quantifying production of certain components of the ECM in tissue engineered cartilage (Park *et al.* 2006).

Computer processing applied to microscopic images of stained cartilage can quantitatively analyze distribution of glycosaminoglycan (GAG) in cartilage. Staining tissue sections with safranin-O produces a red color. The intensity of this color in the microscopic images can be quantified and is proportional to the percentage of wet weight that GAG accounts for. Comparing the intensity of this color in low resolution microscopic images can be used to compare GAG densities and distribution between natural and tissue engineered cartilage (Martin *et al.* 1999).

2.4.3 – Non-Destructive

Non-destructive and minimally invasive analysis techniques are currently being explored for use in many tissue engineering applications. Side viewing fiberoptic probes can be inserted into tissue engineered constructs or incorporated into scaffolds as the tissue is being cultured. By exciting and measuring fluorescent emission of tagged cells it is possible to confirm viability of inner cells while leaving the majority of tissue intact. The advantage of side viewing fiberoptics is that the probe can be rotated to excite cells and simultaneously image them around the probe instead of being limited to only being able to image the cells in front (Lima 2004).

Ultrasound is also a novel technique when applied to analysis of tissue engineered constructs. This imaging modality can be used to determine if the tissue is homogenous throughout its composition, and it is also sensitive to biochemical indications of healthy cartilage which can be compared with ultrasound data from natural menisci. Other advantages of ultrasound include its relative inexpensiveness when compared to other medical imaging modalities, it doesn't use radiation, and the equipment is often portable. However a big drawback of ultrasound is that it requires a lot of training to be able to produce good images (Shull, Chapter 3). For biomedical applications including imaging of tissue engineered cartilage, a transducer would be used to produce a frequency greater than 40 MHz. This frequency provides sufficient depth, 5 to 6mm, for current tissue engineering applications as well as the ability to characterize the tissue in terms of its biochemistry and fiber orientation (Hattori *et al.* 2003).

2.5 – Cell Culture

2.5.1 – Overview

The primary cells which produce cartilage are called chondrocytes. There are three major types of cartilage: elastic cartilage, hyaline cartilage, and fibrocartilage (Mow *et al.*, 2005). Each is characterized by the composition of its extracellular matrix, or ECM. The ECM of cartilage is essentially a proteoglycan gel suspending a dense network of protein fibers (Mow *et al.*, 2005). The properties of these fibers are dependent on the cartilage type. Elastic cartilage is mainly composed of elastin and forms external cartilaginous tissues such as the ear, while the fibers of both hyaline cartilage and fibrocartilage are formed by different types of collagen, types II and I, respectively (Hall, 2005; Mow *et al.*, 2005); Hyaline Cartilage covers the surface of joints and

primarily serves to reduce friction, while fibrocartilage is found in the meniscus, ligaments, tendons, and the spinal discs (Hunter, 2011). The primary cell type for all types of cartilage is chondrocytes. Fibrocartilage-producing cells are further classified as Fibrochondrocytes, because their morphology differs slightly from the others and have some characteristics of fibroblast cells (Mow *et al.*, 2005). There are three major methods to culture chondrocytes: primary cells, mesenchymal stem cells, and carcinoma-derived cells.

2.5.2 – Primary Chondrocytes

Ideally, chondrocytes from a primary animal source would be used (i.e. meniscal tissue, spinal discs, ligaments, or tendons). These primary cells are the closest one can get to the actual tissue found in the meniscus. However, there are several problems with these cells. These are terminally differentiated cells, which make them difficult to culture *in vitro*, and they will die off once reaching their Hayflick limit (Mo *et al.*, 2009). Additionally, there is a large cost associated with maintaining the animal and with harvesting the chondrocytes each time they are needed for an experiment, and the chondrocytes begin to lose their cartilage-like phenotype when grown in a traditional monolayer culture (Tsuchiya *et al.*, 2004).

2.5.3 – Mesenchymal Stem Cells

A more recent and attractive option is the use of stem cells, specifically mesenchymal stem cells. Mesenchymal stem cells are the progenitors to a number of tissues, including bone, cartilage, adipose, muscles, tendons, and ligaments (Chamberlain *et al.*, 2007). Unlike primary chondrocytes, MSCs can be cultured for long periods of time in an undifferentiated state, and then transformed into the desired cell lineage via media conditions (Chamberlain *et al.*, 2007; Mow *et al.*, 2005; Tsuchiya *et al.*, 2004). However, the traditional source of MSCs, bone marrow, appears to lose its ability to specifically form chondrocytes the longer the cells are kept in an undifferentiated state (Tsuchiya *et al.*, 2004). Additionally, it can be difficult to derive the correct cell line from MSCs, since there is no one canonical protocol for differentiating the cells and the differentiating capacity can be influenced by a number of variables, including cell source and time spent in culture and the source of the MSCs: for example, it may be more difficult to induce chondrogenesis in adipose-derived mesenchymal stem cells (Chamberlain *et al.*, 2007; Liu *et al.*, 2009; Tsuchiya *et al.*, 2004). In the past decade, mesenchymal stem cells have been isolated from synovial tissue in joints (Fan *et al.*, 2009). These Synovial MSCs are believed to have a much higher chondrogenic potential than MSCs derived from other tissues, and there

have been several studies into their chondrogenic potential (Fan *et al.*, 2009; Varshney *et al.*, 2010; Katagiri *et al.*, 2013). However, all of these studies isolated the synovial MSCs from a primary source, and there do not appear to be many commercially available cell lines. Some studies have looked into getting past the difficulties of both correctly differentiating mesenchymal stem cells and with culturing primary cells by co-culturing both cells, testing the hypothesis that the primary chondrocytes will influence the differentiation of the mesenchymal stem cells (Mo *et al.*, 2009; Tsuchiya *et al.*, 2004; Varshney *et al.*, 2010).

2.5.4 – Cancer-Derived Cells

The third option is to use a cancer-derived cell line. The two major drawbacks of using a cancerous cell line are that the cells cannot be used in an animal model and sometimes show very unusual cellular characteristics due to mutations. Additionally these cells are unusable for a clinical application because they are derived from cancer. However, these same unusual cellular characteristics can lead to cell lines with properties that are normally difficult to obtain and the cell line can typically divide indefinitely, unlike both primary cells and mesenchymal stem cells. Research was conducted on two mouse cancer cell lines: C3H/10T1/2 and ATDC5. C3H/10T1/2 cells were derived from an embryonic sarcoma, have a fibroblastic morphology, are a good transfection host (meaning they could be infected with a cell-viability marker), and have shown the ability to differentiate into type II collagen-producing chondrocytes (Denker *et al.*, 1999; Haas *et al.*, 1999). However, the cells are only usable for experimentation between passages 5-15, or ~50 days, which makes them unattractive for studies that will require culturing over a longer time frame (C3H/10T1/2). This eliminated C3H/10T1/2 as a choice, since a longer time period will be required to expand the cells sufficiently for our experiments. The second cell line, which is being used in this study, is ATDC5, a chondrogenic cell line derived from an embryonic teratocarcinoma that has an epithelial-like morphology (Shukunami *et al.*, 1996, 1997; ATDC5). It can be maintained in an undifferentiated state, and when treated with specific growth factors will sequentially differentiate into cartilage and then bone (Shukunami *et al.*, 1997; Yoshikawa *et al.*, 2013). However, the progression into bone can be chemically inhibited by treatment with parathyroid hormone or an iron overload which leave it in a chondrogenic state (Shukunami *et al.*, 1996; Ohno *et al.*, 2012).

2.5.5 – Growth Factors for Chondrogenesis

One of the major issues with culturing chondrocytes is that, even if the correct cell type is obtained, chondrocytes begin to de-differentiate when grown in traditional cultures (Tsuchiya *et al.*, 2004). There has been extensive research into the different factors which induce chondrogenesis and maintain cell phenotype. In 2008, Johns and Athanasiou studied the effects of five growth factors on the collagen production and differentiation of coastal chondrocytes (isolated from a rib) and found that treatment with insulin-like growth factor I increased cell-number and induced a fibrocartilaginous morphology (John, 2008). Several studies have examined the effects of the Bone Morphogenic Protein family on cartilage regeneration and differentiation of stem cells with results pointing to BMP-2 and -4 having the capability to induce chondrogenesis in MSCs (Kuroda, 2006; Sekiya, 2005; Steinert, 2003). Several studies have also looked into using the family of Transforming Growth Factors, specifically the varieties TGF- β , to induce differentiation with mixed results: some studies say that the use of TGF- β caused differentiation, while other studies claim it had no effect (Johns *et al.*, 2008; Kuroda, 2006; Sekiya, 2005; Varshney *et al.*, 2010). Lastly, Angele *et al* has conducted studies on the effects of environmental mechanical stimulation, through both hydrostatic pressure changes and compression, and determined that cyclic mechanical stress increases mesenchymal stem cells' chondrogenic capability (Angele, 2003, 2004).

3 – Project Strategy

This project explores the possibility of growing a cartilaginous thick tissue culture by seeding a 3D printed, biodegradable scaffold with a chondrocytic cell line. The following chapter outlines the objectives and constraints of our project as well as the approaches used to obtain them.

3.1 – Original Client Statement

Each knee joint has two, three-dimensional cartilaginous structures that provide shock absorption, stability, and lubricity to the knee; the lateral and medial menisci. Meniscal tears and ruptures are common injuries that often experience difficulty healing. The team will engineer a three-dimensional, biomorphic tissue scaffold to research the ability to grow, *ex vivo*, replacement menisci. This scaffold will be printed with a commodity 3-D printer modified and re-engineered as necessary by the team to provide higher resolution.

3.2 – Objectives

Through a combination of team discussion, background research, and review of the initial client statement, we were able to determine the projects objectives and constraints. The five main objectives of this project include maintaining proper geometry, cell viability, rapid production, biodegradability, and sterility of the scaffold design. An objectives tree, shown in Figure 3, outlines the objectives and their sub-goals.

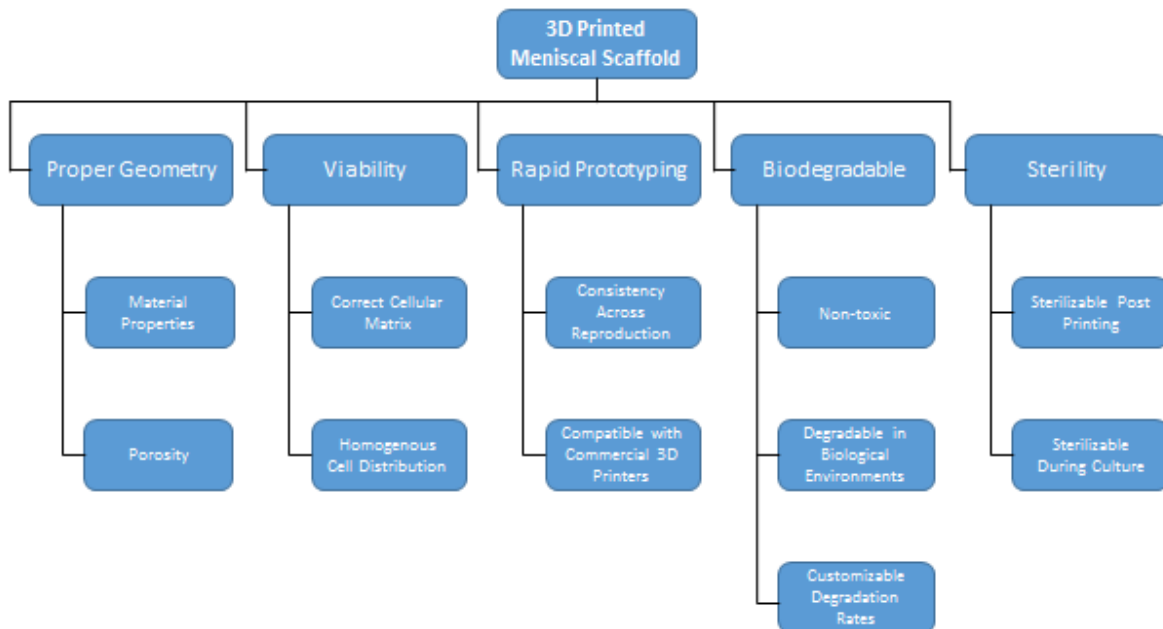


FIGURE 3: OBJECTIVES TREE

3.2.1 – Objectives Overview

- Proper Geometry:** Final scaffold must generate a tissue with the correct geometrical biomechanical properties. The material properties and porosity of the scaffold will dictate cell growth and viability.
- Viability:** The thick tissue culture should be viable in terms of histology and free from necrosis. In order for the design to be deemed successful, the tissue engineered construct should contain viable cells throughout all layers of the scaffold.

- **Rapid Production:** Must be able to quickly generate scaffolds with a commercial 3D printer. Additionally, the scaffold structure should be consistent across multiple printings and different types of printers.
- **Biodegradable:** Scaffold must be non-toxic and degradable in a biological environment. The degradation rate of the scaffold will be tailored to tissue growth by material selection.
- **Sterility:** Scaffold must be sterilized after printing and during culturing. Ideally, the scaffolds would be in a controlled, sterile environment while printing but due to the scope of this project and laboratory limitations, sterilization of scaffolds after printing and before culturing should be sufficient.

3.2.2 – Quantifiable Objective Comparison

After defining and outlining the objectives for this project, a quantifiable method must be used to compare their importance. A Pairwise Comparison Chart (PCC) is used to determine the importance of each objective relative to one another. The PCC in the table below quantifiably compares the objectives outlined in the previous section. Upon completion of the PCC, the group determined that cell viability and ensuring proper geometry, with scores of 3.5 and 3 respectively, were of utmost importance for this project’s final scaffold while biodegradability, sterility, and rapid producibility were then ranked less important in that order. The results from the PCC refocuses the scope of the project and determines what objectives must be fulfilled and which may be sacrificed in the project’s development.

TABLE 3: PAIRWISE COMPARISON CHART

	Proper Geometry	Viability	Rapid Production	Biodegradable	Sterility	Total
Proper Geometry		.5	1	1	.5	3
Viability	.5		1	1	1	3.5
Rapid Production	0	0		0	0	0

Biodegradable	0	0	1		.5	1.5
Sterility	.5	0	1	.5		2

3.3 – Constraints

The group identified four constraints they must consider when moving forward with this project. These constraints include:

- accurate 3D printer fidelity
- usage of a non-human cell line
- non-destructive cell viability testing
- costs within budget

The 3D printer must be able to accurately print a scale at a scale of 2/10 mm. Acquisition of human cells for viability testing is beyond the capacity of this project and the group is limited to ATDC5 mouse chondrocytes.

Viability testing is both an objective and a constraint due to the need to test for cell necrosis without destructive testing. We must develop a nondestructive test to determine the cell viability within the core of the scaffold. The budget for this project is approximately \$550. The initial cost for the MakerBot® was \$2500, while the costs for our chosen cell line and viability testing kits are approximately \$650. Our budget must be limited to printer modifications and the purchase of the polymers used to create our scaffold. Additionally, a combination of computational limitations, hardware malfunctions, and time constraints served to limit the scope of this project to a “proof of concept.” Rather than attempting to reproduce the geometric and mechanical properties of the meniscus, The team focused on generating a 3-Dimensional Scaffold which could grow viable thick tissue cultures that could in the future be used as a basis for meniscal regeneration.

3.4. Revised Client Statement

The team will engineer a three-dimensional, biomorphic, biodegradable, biocompatible tissue scaffolds and research the scaffolds ability to grow, *ex vivo*, thick tissue culture which can proliferate and differentiate cells beyond the typical nutrient penetration barrier. This scaffold

will be printed with PLA on a commodity 3-D printer, modified and re-engineered as necessary by the team to provide higher resolution.

3.5 – Project Approach

The purpose of this study is to generate a biodegradable scaffold which can be seeded with cells and used to grow thick tissue culture *in vitro*. Porous scaffolds with differing geometries will be generated for experimentation with cells. These scaffolds will be composed of PLA so that the scaffolds will be biodegradable and printable on the 3D printer. The effect of porosity and shape on thick tissue culture success will be determined through multiple experiments with cell culture.

The cell line to be used is ATDC5. Experiments will be conducted to optimize the cell line's differentiation into the cartilage producing cells, chondrocytes and fibrochondrocytes. Once the ideal conditions for culturing/differentiating ATDC5 cells are determined, the cells will be seeded onto the porous scaffolds using a collagen hydrogel. The amount of hydrogel, amount of cells, and cross-linking method will need to be optimized.

Given the budget and time allotted for this major qualifying project, some aspects need to be simplified for the group to establish a proof of concept. Instead of designing and constructing a bioreactor to increase nutrient perfusion, the seeded scaffolds will be cultured on a shaker table inside the incubator. This agitation will help nutrient perfusion as well as allow the geometry of the scaffold to be the limiting factor. This allows the success of the tissue engineered construct to be dependant on the scaffold geometry more than the bioreactor it was cultured in.

Once we have seen that cartilage (cell differentiation?) has been grown, it will need to be histologically tested. In addition to the viability testing during and after culture, some of the biological structures will be cryogenically frozen and sectioned with a microtome. Different histological tests will be performed and this will allow for microscopic analysis of the distribution of internal cells.

3.6 Biocompatible material

The 3D printer that was initially used for this project was the MakerBot® Replicator, a commercially available dual extrusion printer. The Replicator can print a variety of different filaments that include polylactic acid (PLA), polyvinyl alcohol (PVA), and acrylonitrile

butadiene styrene (ABS). As the project moved forward the group began to use a Replicator 2 as the main printer for the printing of all scaffolds. The Replicator 2 can print using the same types of filaments as the Replicator. As required for this project the material used in printing the scaffold must be biocompatible and biodegradable. ABS is neither biocompatible nor biodegradable and will not be used for this project.

4. Methods and Design Alternatives

This project contains many parts and is very multi-faceted. It combines elements of mechanical engineering for the 3D printer work, computational design for designing the scaffold and working with the printer software, biology for the cell culture, and biochemistry for histological analysis. The team therefore incorporated an extensive amount of methodologies and possible designs/protocols into the project. These methods and alternative designs are discussed in the following chapter.

4.1 3D printer modification

4.1.1 MakerBot® Extruder Nozzles

The Replicator is commercially available with extruder nozzles that can extrude filament at a size of .4 mm. Smaller size nozzles are not commercially available from the MakerBot® company and must be either purchased from other companies or custom made. This presents a problem to achieve an optimal tissue ingrowth and proliferation, which occurs when a scaffold design has pore sizes ranging from 200 - 400µm and having a 50% void fraction (Hsu, *et al.* 2011; Tareoka, *et al.* 2010). This pore size cannot readily be achieved using the standard .4mm replicator nozzle and smaller nozzles, with diameters of .2mm or .25mm, will have to be acquired. A previous MQP group that had worked on a similar project had acquired CAD drawings of custom designed nozzles from MakerBot® and had multiple nozzles machined at the WPI machine shops for use with the Replicator. The team would use the original set of extruders that had been custom made and would also acquire the CAD drawings for the creation of more nozzles for any further testing.

4.1.1.1 Acquiring Smaller Extruder Nozzles

The team initially looked at having different outside machining companies either create the extruder nozzle blanks, which would then be sent to a company for drilling, or create the

extruder nozzles and drill them as well. Multiple companies were looked at to machine the extruder blanks but none were able to manufacture the extruder blanks.

Since an outside company was not able to machine nozzle blanks for the project the group registered the project with the Washburn Shops here on campus. The CAD drawings of the nozzles were sent in with the groups' registration and all that was left to do was to wait for the registration to go through with the Washburn Shops. The group was finally contacted by our appointed staff member in Washburn Shops but after sending an initial email we heard no word back about moving forward with getting any nozzles machined on campus. It was at this point in the project that it was becoming apparent that the group would have little time to machine and bore new nozzles and that our primary focus would need to be on the printing of scaffolds.

After talking with Jessie Halter, a member of a previous MQP group, the group was directed to a website called www.qu-bd.com. This website sold extruder nozzles compatible with the Replicator. The group then purchased four nozzles with a orifice diameter of .25 mm. Two of these nozzles would be used for printing purposes while two could be set aside for any further printer modifications. This will allow the group to perform any experimentation with the nozzles to increase the resolution of the final print, time permitting. For the duration of the project the nozzles used with the Replicator were the .25 mm nozzles acquired online from www.qu-bd.com and the nozzles used by the previous year's MQP.

4.1.2 MakerBot® Replicator Problems

During the course of printing scaffolds, problems with the printer began to occur and the group was initially unable to determine the source of these problems. We initially believed that the print settings of our scaffolds needed to be optimized for the prints to be successful. Modifying the print settings did not lead to a successful print, even when print settings from a previously successful MQP were used. These failures prompted the group to look at other reasons for why the prints were failing and initial ideas were that the extruders needed to be cleaned. Upon subsequent cleaning two problems were noticed by the group; one, that a small Delrin plunger responsible for pushing the filament up against the actual extruder was not working properly, and two, that a small piece of the printer that caused the extruder to rotate properly was loose within its housing.

To keep the small piece of the printer secured in the printer, it was re-tightened into the drive shaft. This solved the problem of the extruder not rotating properly when the printer was running during a print. Solving the problem with the Delrin plunger proved to be harder than expected as that part of the printer was no longer available for purchase anywhere. The Delrin plunger is a small piece of the Replicator that pushes filament up against the extruder and causes the filament to get caught and pushed into the extruder nozzle. If this part is not functioning properly then no filament will actually extrude during a print. This part is made of an easily degradable polymer and will become worn down after a period of use in the Replicator. Since no new Delrin plungers were available for purchase the group 3D printed replacements. .STL files for the part were found on www.thingiverse.com and two plungers were printed using other 3D printers found on campus.

These printed parts were not the same quality as the original prints and had to be slightly modified to try and get them to work properly when placed within the printer. These replacement plungers worked initially but filament extrusion was slow compared to when the original plunger was working properly and filament extrusion seemed to stop at different point during a print. An alternative method of fixing the problem with the extruder was researched and it was found that an extruded upgrade kit was available for purchase online. This upgrade kit replaced the Delrin plunger entirely with two solid steel rollers that would push the filament through the extrusion nozzle using a spring tension system. This upgrade kit was successful in extruding filament during a print but the prints continued to fail during the printing process. It was at this time that it was decided that acquiring scaffolds was a top priority for the team and that alternative methods of printing scaffolds should be researched.

4.1.2.1 Alternative Printing Methods

The group began asking around campus to discover if there were 3D printers they could use to print scaffolds. There were two 3D printers in the Mechanical Engineering Department but these could not be used as both printers were Objet printers and only printed in resin, a material not suitable for use in a biodegradable scaffold. The group visited the WPI Collablab, as it was known that members of the organization worked with 3D printers, but discovered that the printers built by members of Collablab were unable to print at the desired resolution of this project.

After discussing the need to find a better 3D printer with another MQP group it was discovered that Professor David Planchard was in possession of two Replicator 2 printers. Professor Planchard was approached about the possibility of using his printers to print scaffolds and he agreed, we only had to bring him an SD card with our scaffold files that we required to be printed. The team was able to acquire multiple scaffolds with Professor Planchard's help before he could no longer let us use his printer, as he required both printers to finish his MQPs.

While the team used Professor Planchard's printers to print scaffolds we continued to look for other means of producing scaffolds for when we would no longer be able to use those printers. A member of our team was put in contact with Cathy McEleny at Draper Laboratories. The team was told that they would be able to help us print more scaffolds and it was learned that a Replicator 2 was available for use at their Rapid Prototyping Center in Boston. Two members of the team traveled to Draper Laboratories and were successfully able to print scaffolds after modifying the print settings. The team plans to continue visiting Draper Laboratories to print more scaffolds for use in future cell seeding tests.

4.1.3 MakerBot® Software

Before any of the scaffolds could be printed all the CAD files needed to be converted to a specific type of file known as an .stl file. Any object that contains a circular or rounded section cannot be properly printed by a 3D printer, as the printer deposits material along a series of points and anything that is rounded can have an infinite number of points for the printer to calculate for. Creating an .stl file resolves this technical problem by converting the entire CAD file into a set of triangles that 3D printing software can use to calculate the route the filament extruder will take while depositing material. The smaller the amount of triangles generated in the .stl file the "coarser" the final printed object will be while a larger amount of generated triangles will increase the quality of the final print.

Once these .stl files have been created they are then used to generate a specific code that the 3D printer will use to print the scaffold. There are a multitude of softwares that can be used to generate these codes and MakerBot® Replicator accepts codes generated by three different types of software, Thing-O-Matic, ReplicatorG, and MakerWare. Going off the advice of Nick Trebucco, the one who allowed the group to use his printer, we used to ReplicatorG as the

software to generate our printing code, or G-code as it is called when using that specific software. The version of the software used for this project was ReplicatorG 0037.

ReplicatorG offers a variety of printing options which can be modified to alter the final printed object. The printing options that can be modified using ReplicatorG are separated into sections; general settings, plastic, and extruder, as well as general options for the creation of the G-code. For the general options there is the choice to choose which extruder will be used during the print, either the right or the left extruder, whether to use a raft or support for the print, and whether to use ReplicatorG default start and end code or whether to Print-O-Matic code generation. During this project both the right and left extruder were used as we modified the printer and no supports or rafts were needed during the printing of the scaffold. The default start and end code were used for the G-code as the Replicator used for this project did not use stepper extruders.

The settings section of ReplicatorG is where the most modifications can be done to the G-code used to print an object. The settings that can be modified include object infill, layer height, number of shells, feed-rate, and travel feed-rate. The object infill setting will determine the final density of the print, with an object infill of 100% leading to a completely solid object, while an object infill of 0% will print a hollow object. Layer height determines the width of each layer of filament that is laid down by the printer during a print. The default layer height is .27 mm in ReplicatorG software. The number of shells refers to the thickness of the printed object. Every object automatically has one shell for its initial thickness and each additional shell adds to the thickness of the final print. The feed-rate and travel feed-rate deal with how fast the extruder travels, either when the filament is being extruded or when the extruded is moving between extrusions. Feed-rate is the speed at which the extruded moves when filament is being extruded during a print while travel feed-rate is the speed at which the extruder moves while it is not extruding filament. Both feed-rate and travel feed-rate are set in units of mm/s.

For the intended size of our scaffold, being approximately 10 mm x 10 mm x 10 mm, or the corresponding modular sections being approximately 10 mm x 10 mm x 3 mm, there would essentially be no void space, and object infill was set to 100% for the G-code. For layer height we experimented with variable heights, ranging from .2 mm to the standard of .27 mm to see which option would give the greatest fidelity in our scaffold print. The number of shells was

left at the default of one shell for most prints, but zero shells were used upon learning that a previous MQP have achieved successful results with that setting. The default feed-rate and travel feed-rate are to 40 mm/s but we had more success with much slower feed-rates, with our feed-rate and travel feed-rates set in the ranges of 5 - 15 mm/s.

The next two sections that allow for modification of the G-code include changing the filament diameter and extruder nozzle size. Changing the filament diameter in the G-code will determine how much filament is actually extruded from the nozzle. The actual diameter of filament that is used in all MakerBot® 3D printer is 1.75 mm, but the filament may swell slightly due to exposure of moisture in the air over time. The filament diameter is automatically set to a value of 1.82 mm in ReplicatorG to account for this possible swelling and the minute tolerances in the stock filament. Increasing or decreasing this value can affect how much filament is actually fed through the extruder during a print. The greater the value inputted into the G-code the lower the amount of actual filament that will actually be extruded, as the machine will not feed in as much filament to begin with. The lower the inputted value the greater the amount of filament that is extruded, as the machine will believe there is a smaller amount of filament being fed into the extruder and will increase the output to generate the required volume of filament. The final option that can be modified in ReplicatorG is the nozzle diameter. Any value could be entered here and that would help determine the amount of filament that would be extruded during a print.

For this project the filament diameter was tested at values ranging from 1.82 mm, the default setting in ReplicatorG, to 2.10 mm. This was to see which filament setting would allow for an optimal print while creating thinner filament layers.

4.2 Scaffold Design

The main objective for designing the scaffold was creating an optimal geometry which allows continuous nutrient flow to all layers of cells. Previous work conducted by our colleagues (One of the previous MQPs) has shown that biodegradable scaffolds made with high volume, high surface area, 3-dimensional fractal shapes, can provide the required nutrient flow to allow thick tissue culture.

4.2.1 Fractal Generation

Several processes were examined to generate fractal structures for use in the printed scaffold. The first was to directly model fractal-like shapes using a CAD program such as SolidWorks. This was the most straightforward method, but only allowed for the creation of simple fractals such as the Menger Sponge and was very labor intensive. However, this method also allowed for direct modification and manipulation of the scaffold and smooth conversion to the printable STL file format.

A second option was to use a computer program to procedurally generate a fractal that could be converted into a workable CAD file. The converted file could then be modified into the desired scaffold shape and converted into an STL file. The primary advantage of this method is that it allows the user to quickly generate many complex fractal shapes. However, the programs and especially the file conversion can be very processor-intensive, and many of the programs require a good working knowledge of fractal mathematics. The team primarily examined the program Incendia (<http://www.incendia.net>), which is a free 3D fractal generator. The program uses voxels (essentially “3D Pixels”) to generate fractals based on a preset list of fractal equations. The results shapes can be exported as an STL file.

The third option explored by the team involved using open-source, premade 3D fractals available on 3D Printing websites such as www.thingiverse.com. These files have the advantage of being completely pre-fabricated and available in the printable STL format. Because these were “ready-to-print” files, modifying them required the processor-heavy conversion into a workable CAD file. Additionally, these files often contained errors (e.g. features on adjacent faces were not aligned correctly).

4.2.2 Gross Scaffold Structure

While the proper internal scaffold geometry allows the seeded scaffold to sustain viable growth, the overall scaffold shape dictates the shape of the resulting tissue grown from the scaffold. The gross shape of the scaffold should, therefore, resemble the geometry of the lateral meniscus, discussed previously in section 2.2.1 of this report. The fractal-like internal geometry is either imported into a CAD file, as mentioned in the previous section, or is generated directly in the CAD software, first so the gross scaffold shape could then be carved out of the fractal block.

4.2.2.1 File Conversion

All of the fractals generated in Incendia and obtained from open source sites were in the printable STL format. However, this format only contains surface information and is completely unmodifiable in traditional CAD programs. In order to convert these files into a modifiable form, such as a SolidWorks Part (.sldprt), the team examined and designed several conversion protocols.

The SolidWorks add-on Surface Mesh Editor is made to process the data obtained from 3D Object Scans from surfaces into workable solids. The team attempted a number of trials with this add-on, with no success. While the process works for surfaces, it was unable to reconcile the voids and complex geometries of a 3D fractal. Below is a simple example of an STL file generated with OpenSCAD (a code-based CAD program).

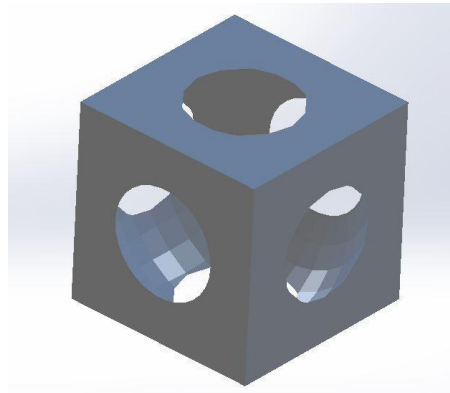


FIGURE 4: SIMPLE "SPHERE-IN-CUBE" GENERATED IN OPENS CAD

When put through the SolidWorks surface mesh process, it becomes one of the following (for the guided and automatic processes, respectively).

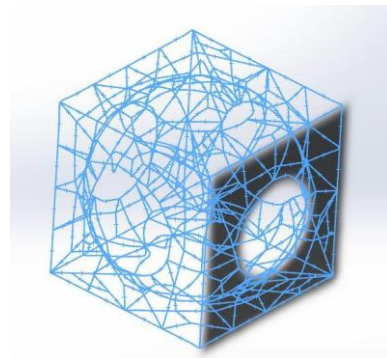
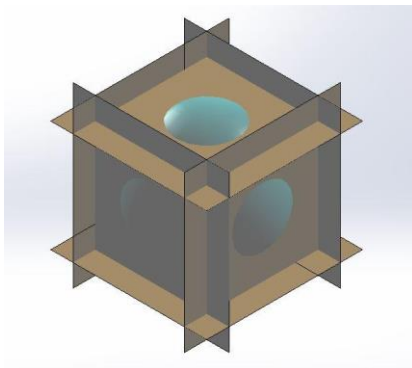


FIGURE 5: ERRORS IN SOLIDWORKS SURFACE MESH CONVERTED. LEFT - GUIDED PROCESS; RIGHT - AUTOMATIC PROCESS

While the object on the right has the right shape, it does not have any editable features, and disappears if the file is reopened.

Due to the issues with the built in SolidWorks processing, the team generated an original protocol using the Autodesk Inventor Surface Mesh Processor, a newly released add on for processing surfaces into solids. The Surface Mesh Processor was used to convert an STL file into an Inventor Part File (.ipt), which was then converted into a .sldprt file so that the time could work with it. While this process worked with moderately complex fractals, it is extremely processor intensive, with total times up to 12 hours. The team eventually decided to use the fractals modelled directly in SolidWorks due to the ease of creation, modification, and processing.

4.3 Alternative Scaffold Designs

The group initially looked at using a third level recursion cylindrical Menger Sponge scaffold design. The third level of recursion would allow for a large surface area to volume ration, which would increase nutrient delivery to cells within the scaffolds core. The group also design a second level recursion spherical Menger Sponge, with spheres being used in place of cubes to connect each pore. Spheres and cylinders were used in these designs to remove the straight surfaces that are prevalent in a typical Menger Sponge fractal. Cells do not grow well on either sharp surfaces and this necessitated the change of design of the Menger Sponge. A custom designed Menger Sponge was also created by the group as another design alternative. This scaffold design was a second level recursion cylindrical Menger Sponge design with modified pores sizes.

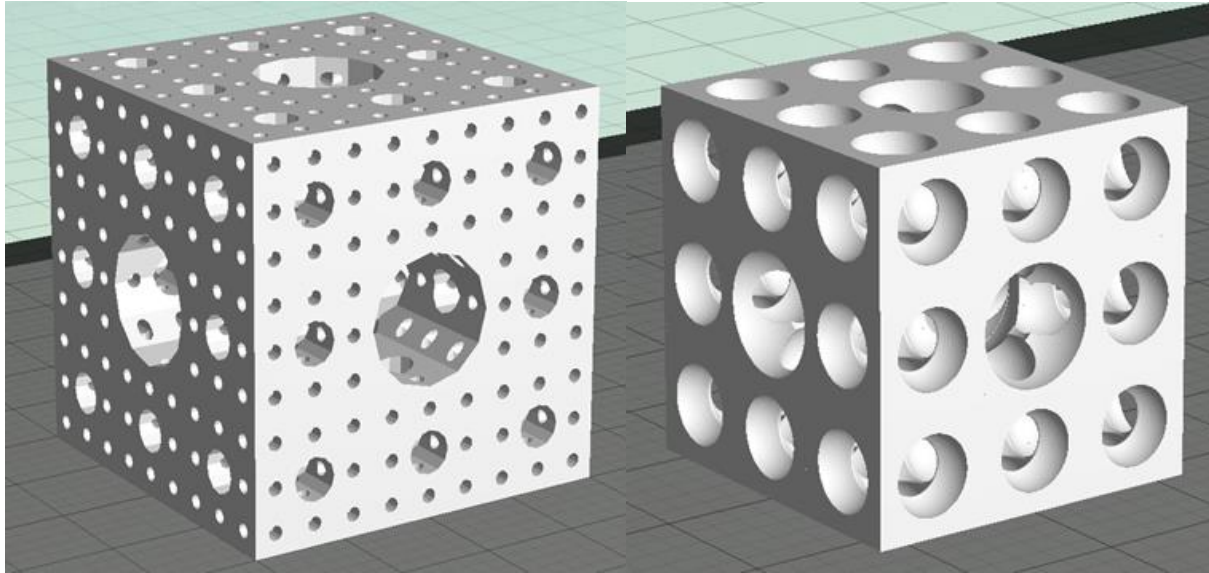


FIGURE 6: DIFFERENT MENGER SPONGE FRACTALS. LEFT - 3RD LEVEL MENGER SPONGE; RIGHT - 2ND LEVEL MENGER SPONGE

When trying to processing the third level recursion cylindrical Menger Sponge the group did not have enough computational overhead and was unable to print that design. This necessitated the group to begin working with the second level spherical Menger Sponge in the hopes that the group would have enough computational overhead to process the design. This design was successfully processed but the team was unable to successfully print the scaffold to completion. Working with the second level recursion cylindrical Menger Sponge the group was able to successfully process and print the scaffold design.

4.4 PLA Degradation Methodology

In a similar way that errors in printing can result in more texture in the scaffold, the way each scaffold degrades over time can result in more texture and be beneficial to the design as a whole. To test this PLA scaffold cubes were weighed and submerged in distilled water. These cubes were maintained at 37° C and removed from the water on days 1, 7, 14, 21, and 28. Testing the degradation of this material over the timeframe of the ATDC5 cells is important for planning the scaffold seeding methodology.

4.5 ATDC5 Differentiation Protocol

The ATDC5 differentiation protocol begins with supplementing the maintenance media with ascorbic acid for 7 days. This addition of this to the media allows the cells to create more collagen in the extracellular matrix. Growing the cells in the presence of this increased levels of

collagen differentiates them into pre chondrocytes. The ascorbic enhanced media components and concentrations can be seen in the table below.

TABLE 4: ASCORBIC ACID ENHANCED ATDC5 MEDIA

DMEM	44%
Ham's F12	44%
Fetal Bovine Serum	10%
Penn/Strep	1%
Glutimax	1%
Ascorbic acid	37 μ g/ml

The final step in the differentiation process is the addition of insulin to the ascorbic enhanced media. The ATDC5 prechondrocytes are culture in this media for 21 days which differentiates them into the final chondrocytes. At some point in the differentiation process the cells will stop dividing when they are fully differentiated. The final differentiation media components and concentrations can be seen in the table below.

TABLE 5: ATDC5 DIFFERENTIATION MEDIA

DMEM	44%
Ham's F12	44%
Fetal Bovine Serum	10%
Penn/Strep	1%
Glutimax	1%
Ascorbic acid	37 μ g/ml
Insulin	10 μ g/ml

4.5.1 BrdU Assay

Bromodeoxyuridine, commonly abbreviated BrdU, is a nucleotide analog which is often used to detect cell proliferation. During the S phase of the cell cycle, DNA is synthesized and BrdU can be incorporated into the new chain in the place of thymidine. Generally cells are exposed to the same amount of BrdU for a set period of time to control the number of cells going through the S phase for each time point. Cells can be fixed after the BrdU incorporated into the DNA, and BrdU specific antibodies allow for the use of fluorescent tags to show newly created DNA in the nucleus of the cells. Comparing the number of fluorescently tagged nuclei to total number of cells shows how many cells are proliferating. Cells were cultured using the ATDC5 differentiation protocol to learn when the cells stop dividing.

4.5.2 Alcian Blue Staining

Alcian blue staining solution (Scytek, pH 2.5) is a common method to confirm chondrogenesis of cells. Alcian blue stains blue for acidic polysaccharides deposited into the extracellular matrix. These acidic polysaccharides include glycosaminoglycans as well as other proteoglycans. Using this for the ATDC5 cell line can determine when in the differentiation process they become chondrocytes which will allow for better planning for the 3D cell culture within the PLA scaffolds. This stain can also be used on the cells within the scaffold to test the final tissue engineered construct for chondrogenesis.

4.5.3 Modified Serum Levels

Given the results of the BrdU experiments that showed half of the cells were still dividing up until the last day of the differentiation protocol, an experiment was devised to explore the possibilities of a modified serum protocol to slow the proliferation of these cells and allow them to differentiate sooner. The modified protocol uses the same media changes, ascorbic concentrations, and insulin concentrations as the standard protocol but at day 7 the fetal bovine serum is reduced from 10% to 2% with an additional 2% adult horse serum. The table below shows the components and concentrations of ATDC5 modified differentiation protocol with lowered FBS and AHS.

TABLE 6: ATDC5 DIFFERENTIATION MEDIA WITH REDUCED FBS AND 2% AHS

DMEM	47%
------	-----

Ham's F12	47%
Fetal Bovine Serum	2%
Adult Horse Serum	2%
Penn/Strep	1%
Glutimax	1%
Ascorbic acid	37 μ g/ml
Insulin	10 μ g/ml

On day 10 of culture the media contains no fetal bovine serum and only contains 2% adult horse serum. This media is used for the duration of of the modified differentiation protocol in an effort to slow division of the ATDC5 cells and promote early differentiation. The table below shows the components and concentrations of this media.

TABLE 7: ATDC5 DIFFERENTIATION MEDIA WITH 2% AHS

DMEM	48%
Ham's F12	48%
Adult Horse Serum	2%
Penn/Strep	1%
Glutimax	1%
Ascorbic acid	37 μ g/ml
Insulin	10 μ g/ml

4.6 Hydrogel Protocol

PureCol EZ Gel (Advanced Biomatrix) was chosen as the hydrogel to seed the 3D printed scaffolds. This is due to previous success that the 2012-2013 major qualifying project team had in using it. In their experience the simple protocol let to the creation of a uniform gel and good results from experimenting with it. It is a bovine sourced type I collagen solution which forms a

hydrogel when incubated at 37° C for 90 minutes. Collagen I concentration for this product is 5mg/ml or 0.5%. This is ideal for this project not only because it is simple to work with, but also because a collagen gel should lead to an early or easier differentiation into chondrocytes for the ATDC5 cells selected for the project.

4.6.1 Cellular Distribution Methodology

Given the time it takes the PureCol EZ Gel the form a hydrogel (90 minutes), it is important to consider cellular distribution when developing and improving upon our seeding protocol. A cell and hydrogel mixture was maintained at 25 degrees Celsius, and experimental groups were added to a 96 well plate every 10 minutes and incubated at 37 degrees Celsius to form a gel.

4.6.2 ATDC5 Differentiation in Collagen Hydrogel

The principal behind the ascorbic acid accelerated differentiation protocol is that the cells are able to produce higher levels of collagen which helps them to differentiated into chondrocytes sooner than the standard differentiation protocol. Even though the PureCol EZ gel is a type I collagen compared to the type II that the ATDC5 chondrocytes produce, the growth and differentiation of these cells in the hydrogel will differ compared with how they behave on tissue culture plastic. To test this cells were seeded in the hydrogel along with a control group of cells on tissue culture plastic. Both of these groups were given the ascorbic accelerated differentiation protocol and even before the addition of insulin at day 7 there were morphology changes noted in the cells grown in the collagen based hydrogel. Below is a comparison of the cells in the hydrogel and those grown on tissue culture plastic.

4.7 Scaffold Seeding Methodology

Scaffold, custom printed wells, and forceps used to seed the scaffolds were sterilized through soaking in isopropyl alcohol and exposed to UV light for 2 hours to ensure there would be no contamination while the scaffolds were being cultured. Forceps and plastic scoopulas used to maneuver and remove the seeded scaffolds from the wells the washed with DPBS to remove isopropyl alcohol before being used to handle the seeded scaffolds. The figure below shows the sterilization process before the scaffolds were seeded.



FIGURE 7: STERILIZATION DURING SEEDING PROCESS

Single scaffolds along with modular scaffolds were used for testing. The modular scaffolds were seeded as two separate parts and held together with the hydrogel. Distinct seeding wells for single and modular scaffolds were created to minimize loss of the collagen hydrogel. After sterilization scaffolds were placed in wells and covered with a cell-hydrogel solution. These seeded scaffolds were then transferred to the incubator for 90 minutes at 37 degrees Celsius to form a solid gel. Below is an image of the seeded scaffolds before after they were removed from the incubator.

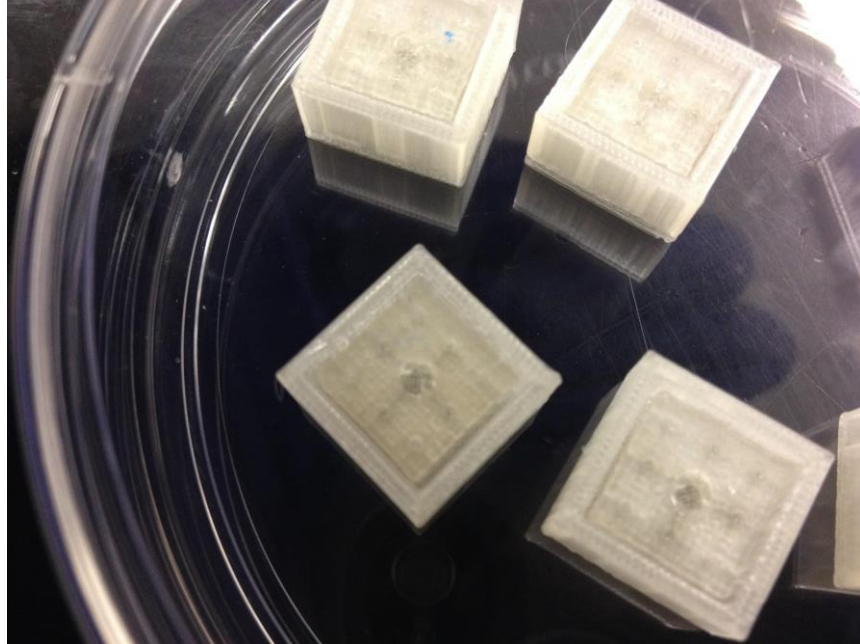


FIGURE 8: SEEDED SCAFFOLDS IN WELLS

Scaffolds were carefully removed from the seeding wells and placed in a 6-well plate which will be used for culturing. Special care was used when removing the modular scaffolds to avoid separating the two halves.

4.8 Tissue Culture Protocol

Seeded scaffolds were covered in media and which was replaced when the color began to change. Based on the results of the reduced serum and collagen gel experiments two media protocols were used to test the final scaffold. Signs of early differentiation in the collagen hydrogel allowed for the reduction in the total culture time for the normal protocol. This protocol included 7 days with the ascorbic enhanced media and a following 15 days in media with ascorbic and insulin. A separate modified serum level protocol was used over the course of 15 days to test the effects of this on cells cells grown in a 3D culture within a scaffold. The image below shows seeded scaffolds covered in media.

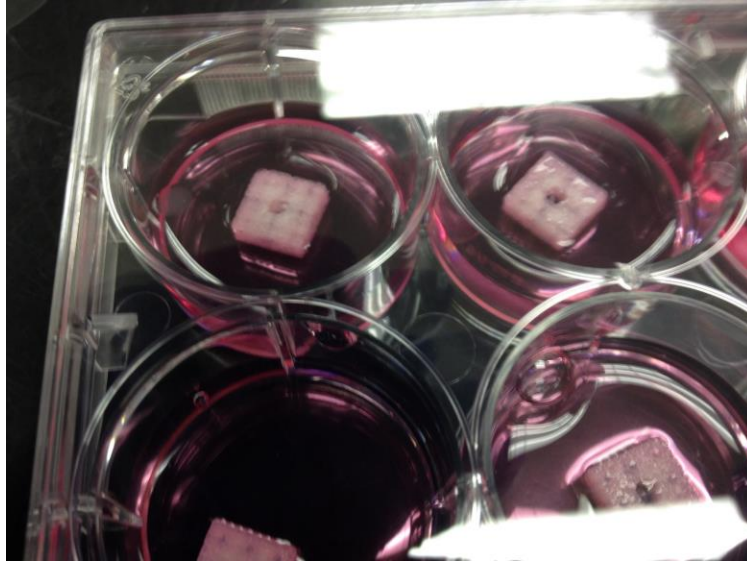


FIGURE 9: SEEDED SCAFFOLDS COVERED IN MEDIA

4.9 Modular Scaffold Protocol

The benefit of seeding modular scaffolds was the ability to section the two scaffold halves and examine the cells on the inner face. This inner face between the two scaffolds is at a depth of 3mm from the surface of the tissue engineered construct. Based on the results of the ascorbic enhanced differentiation protocol in a 2D culture system as well as the 3D collagen hydrogel, the ATDC5 cell line doesn't create large deposits of proteoglycans into the extracellular matrix until the cells have fully differentiated into chondrocytes. Knowing the timeframe within the phenomenon occurs and with the ability to stain and examine cells on the inner surface of the scaffold it is possible to test the viability of cells at a depth of 3mm based on the presence of these proteoglycan deposits.

4.10 Histology Methodology and Testing

Once the cells were cultured in the scaffolds, they were visualized via histological processing and staining. The general procedure for histology involves fixing and processing a sample of soft tissue, embedding it into a block of paraffin wax, cutting 5-10um width slices using a microtome, mounting those slices on glass slides, and then staining the slices. However, due to the large mechanical and chemical differences between the plastic in the team's scaffolds compared to a typical soft tissue, this procedure had to be altered in order to successfully section and visualize the cell-laden scaffold (Finalized Procedure in **Appendix E**). The major issues that had to be addressed were the toughness of the scaffold and adhering the scaffold to slides.

4.10.1 Scaffold Toughness

The experimental scaffolds are essentially 3 components: the plastic Poly-Lactic Acid (PLA), the Collagen Hydrogel, and the ATDC5 cells. While collagen is one of the harder soft-tissues, it can be sectioned using a typical microtome. However, PLA is much harder, and in trials with untreated PLA scaffolds, the microtome was unable to cut sections at all. Instead the PLA was deformed and compressed into the surrounding wax block. In an attempt to soften the plastic, scaffolds were soaked in glacial acetic acid, acetone, or HCL either pre- or post-processing and wax embedment. While no pre-processing had an effect on the plastic's toughness, post-processing soaking in acetone for 2-5 minutes was able to soften several layers of plastic. The team was able to keep the scaffold soft enough to generate 5-6 micron sections by periodically soaking the scaffolds in acetone during microtome sectioning (soaked after every 100-150 microns of scaffold depth cut using the microtome).

4.10.2 Scaffold Adherence to Scaffold

PLA is by nature a hydrophobic biodegradable plastic that undergoes hydrolytic breakdown. During initial histological staining of the PLA sections, no samples successfully remained on the test slides throughout the process. Initially, the team believed that this was due to disintegration of the scaffold, since many histological staining procedures, specifically H&E, involve caustic chemicals such as Xylene and glacial acetic acid; without the surrounding scaffold, the hydrogel seeded gel sloughed off the slides as well.

The team conducted a number of experiments to eliminate the dissolution of PLA. The hematoxylin and eosin solutions used in H&E staining contain a large amount of glacial acetic acid (upwards of 30% in hematoxylin). The team experimented with varying dilutions of the staining solutions (up to 1:10), but scaffolds continued to degrade. Additionally, two water-based stains were used instead, Lite Green and Nuclear Fast Red (NFR). These stains do not incorporate the strong acids required for H&E staining, which makes them a much more viable option for the team's PLA scaffolds. While scaffolds disappeared during this staining protocol, as well, the team noticed an interesting event. During a simple water wash in the NFR procedure, the team observed that entire scaffolds were lifting off of the test slide surface and being lost

during chemical washes. This event was confirmed to also occur in H&E staining, which implies that, rather than dissolving, the scaffolds were dissociating from the test slides

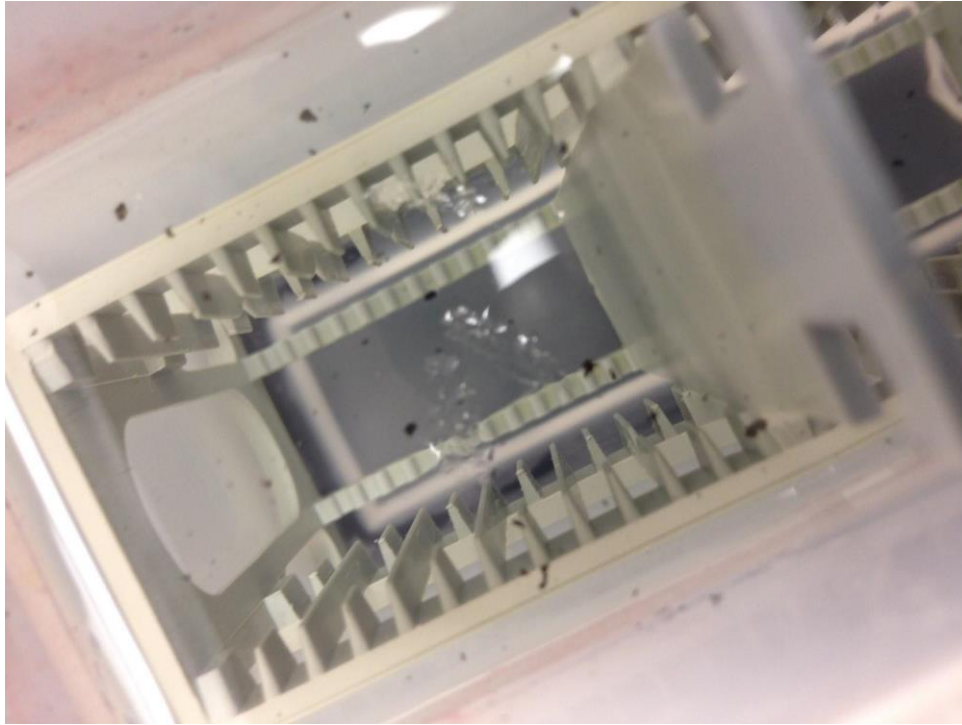


FIGURE 10: PHOTO OF SCAFFOLDS DISSOCIATED FROM SLIDES IN WATER

Several different experiments were run to better adhere the sections to test slides. Scaffolds were embedded in agar blocks in an attempt to stabilize the PLA on the slide and to hold the cell hydrogel in place. However, the PLA detached from the agar during the staining procedure. Sections were also mounted onto Poly-L-Lysine (PLL) slides or uncharged glass slides rather than the typical positively-charged test slides, but this also had no effect. Lastly, the team tried using an epoxy to physically adhere scaffolds to the slides. Two glues were used: Loctite(R) GO2 Glue and Liquid Nails(R) Perfect Glue™. Both glues successfully bonded scaffolds to all 3 slide types; however, only the Loctite(R) GO2 glue on the positively-charged slides was able to survive the Xylene washes used in the staining process. This process allowed the team to continue with histological staining of the scaffold.



FIGURE 11: RESULTS OF GLUE TESTS ON EMPTY SCAFFOLDS. LEFT-RIGHT: H&E STAIN WITH LOCTITE, H&E STAIN WITH LIQUID NAILS, NFR STAIN WITH LIQUID NAILS, NFR STAIN WITH LOCTITE

4.10.3 Scaffold Staining

Visualization of cells in the scaffolds was achieved with several different chemical stains. A modified procedure for Hematoxylin and eosin staining (H&E) was developed for initial visualization of cells from different seeding protocols at varying depths in the scaffolds (Staining Protocol in **Appendix F**). Additionally, several scaffolds slices from the Original and Modified protocols were stained for actin filament using a Phalloidin/DAPI protocol.

5. Design Verification

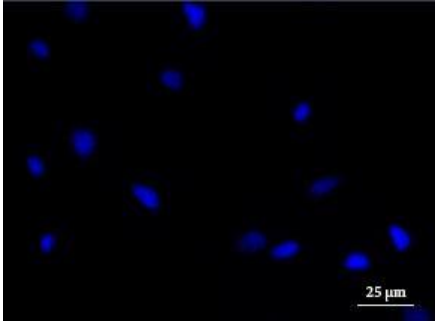
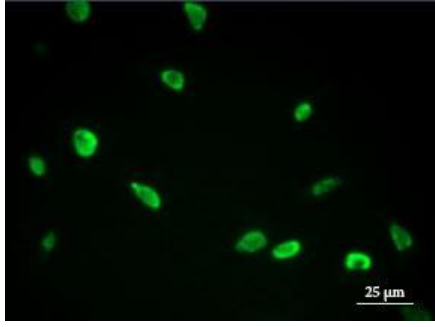
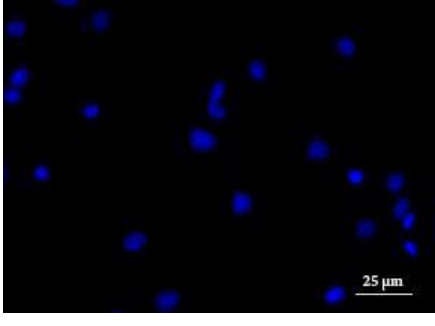
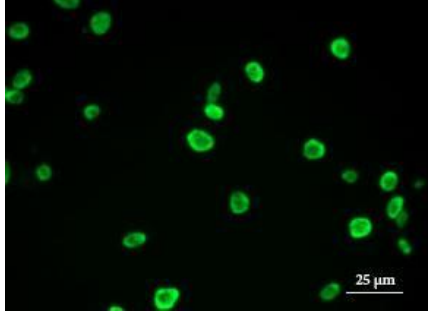
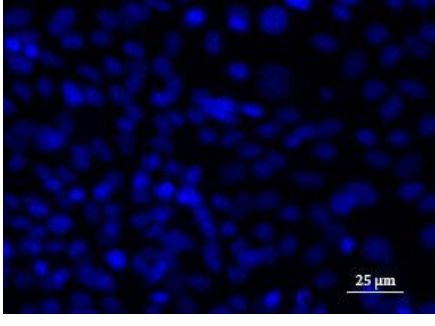
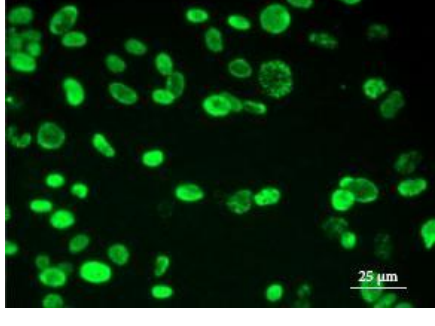
5.1 Cell Feasibility

Before moving on to seed the final design with cells it is important to analyse the results of experiments testing the feasibility of the ATDC5 differentiation and culture system. Results and insights gained from these experiments not only confirm the ability to use this cell type to test the scaffold, but allowed for planning the 3D cell culture and seeding methodology.

5.1.1 BrdU Results

The results of the BrdU assay can be seen below. Hoechst staining results in a blue color for all cells, and cells with BrdU incorporated into the DNA appear with green nuclei. Cells were given BrdU for 24 hours before being fixed and plates were fixed on days 0, 7, 14, and 21.

Comparing numbers of cells which incorporated the BrdU to the total number of cells it was determined that only half of the cells stopped dividing by the end of the experiment. This result needs to be addressed moving forward with this project and taken into account with the 3D cell culture.

Day of experiment	Cell nuclei (40x)	Dividing cells (40x)
Day 0		
Day 7		
Day 14		

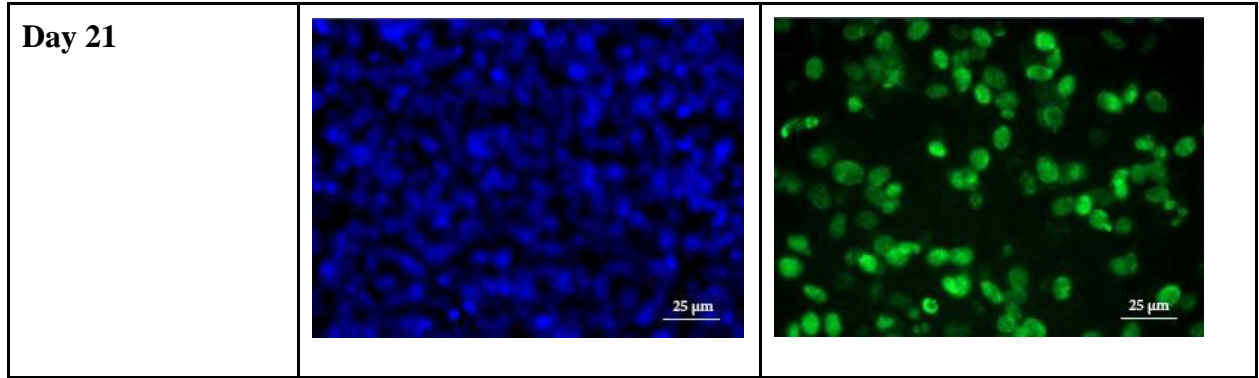
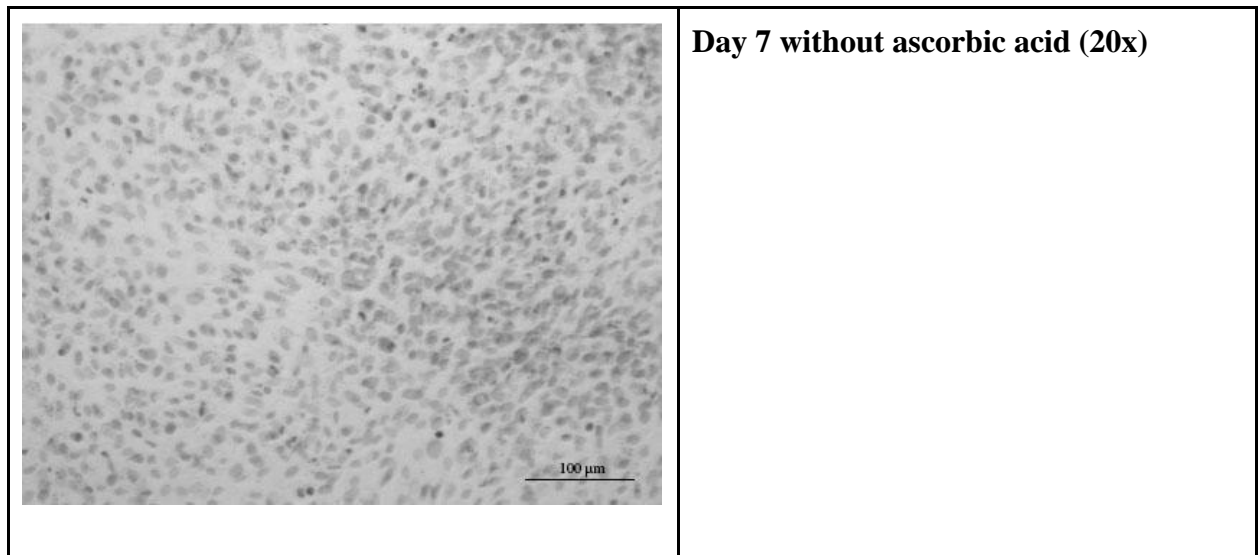
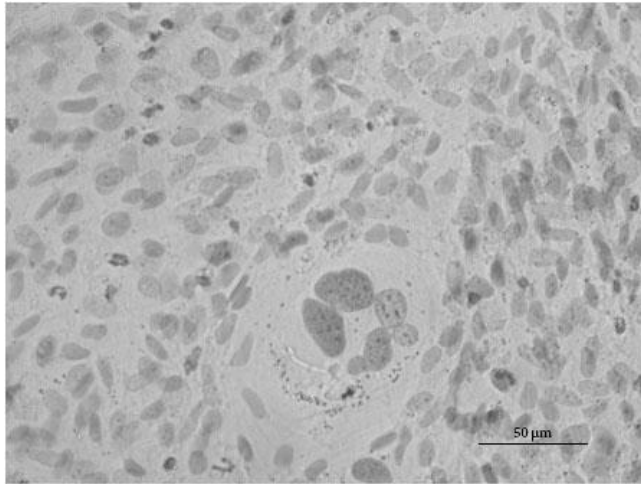


FIGURE 12: RESULTS OF BRDU ASSAY WITH 25μM SCALE BARS

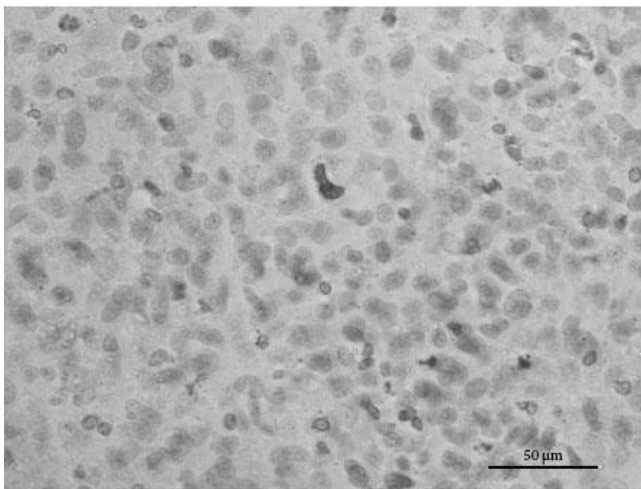
5.1.2 Alcian Blue Staining

The results of the Alcian blue staining on ATDC5 cells throughout the differentiation process can be seen below. Early on in the differentiation of this cell type changes in morphology can be noted but no proteoglycans are deposited. The cells only stain positive with alcian blue later on in the process approaching day 28 of culture.

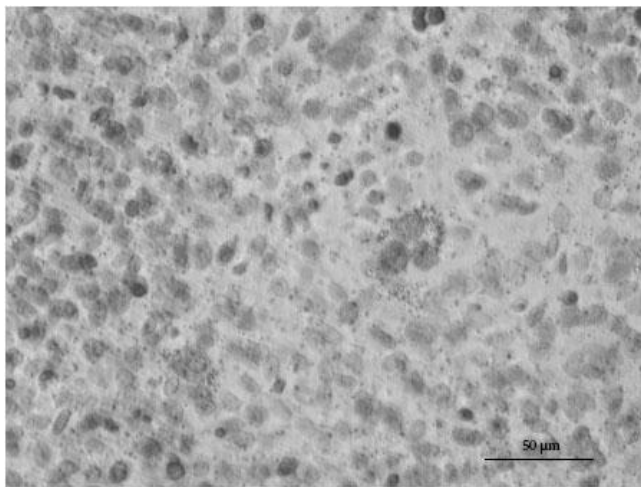




Day 7 with ascorbic acid (40x)



Day 14, or 7 days with insulin (40x)



Day 21, or 14 days with insulin (40x)

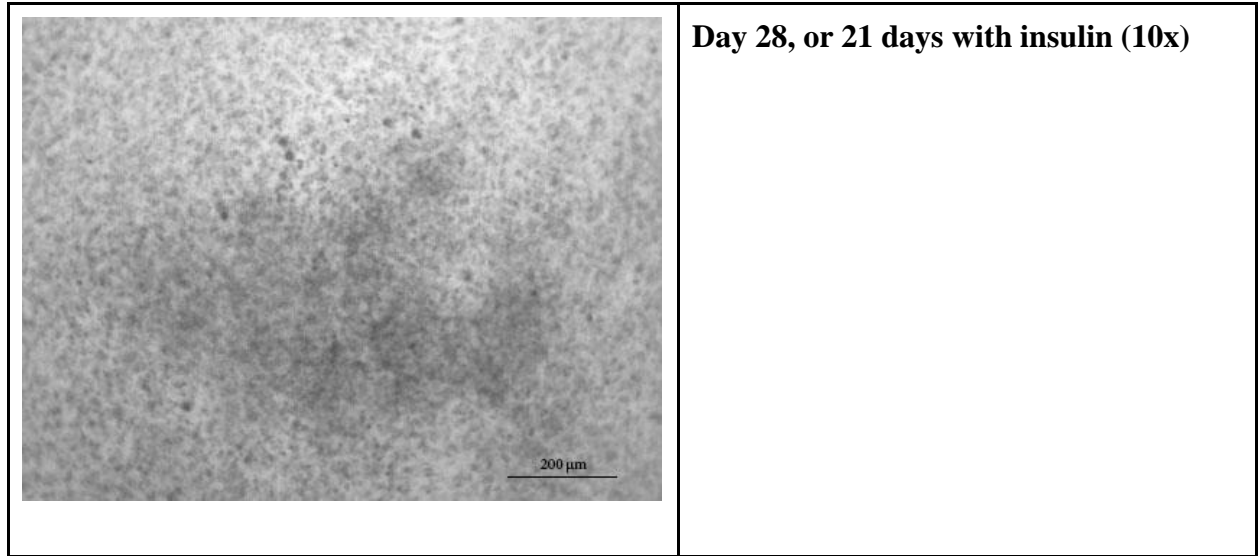
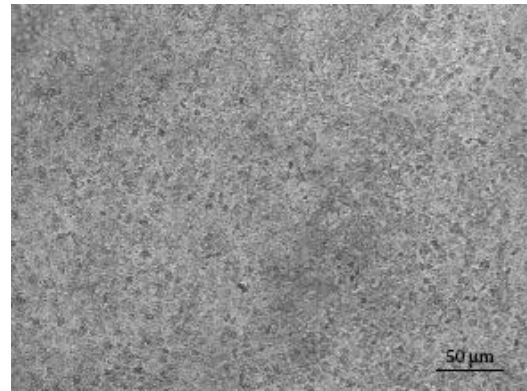
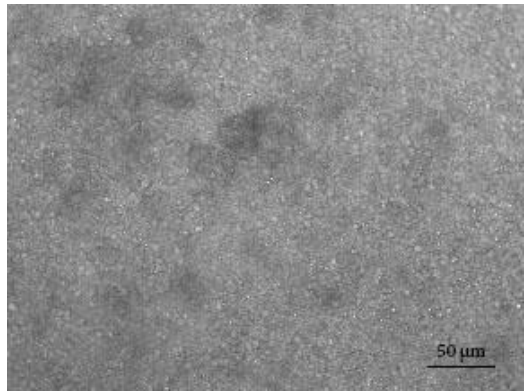
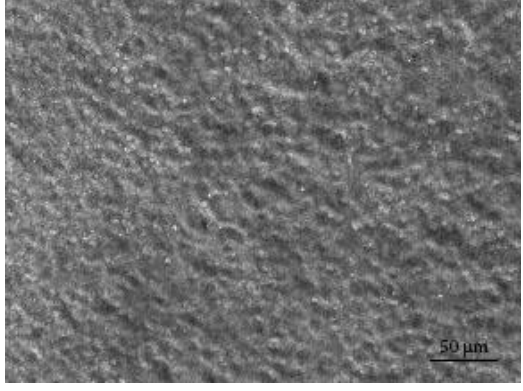
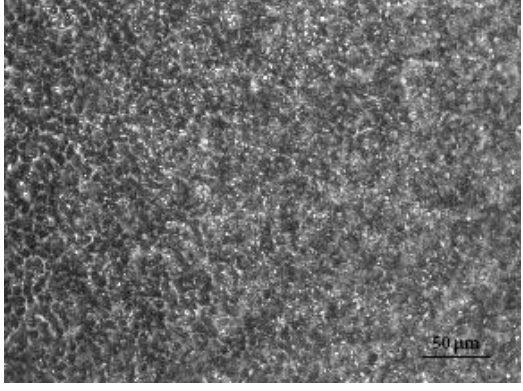
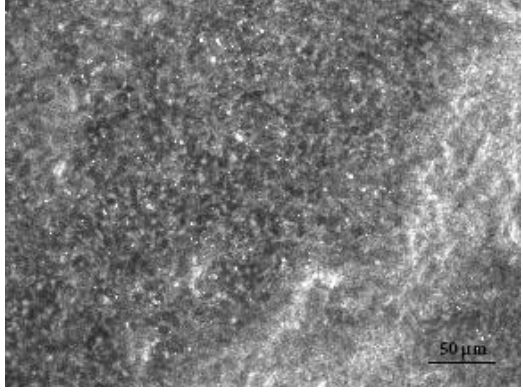
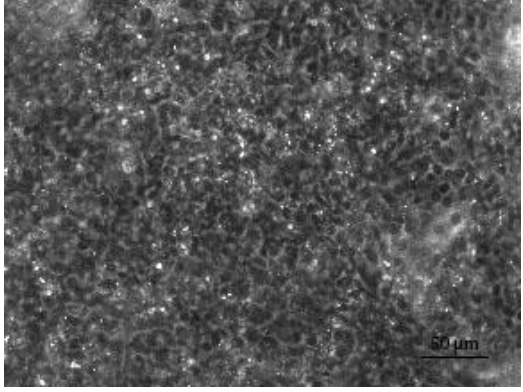
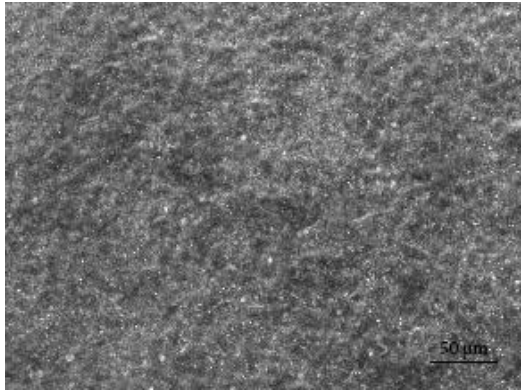
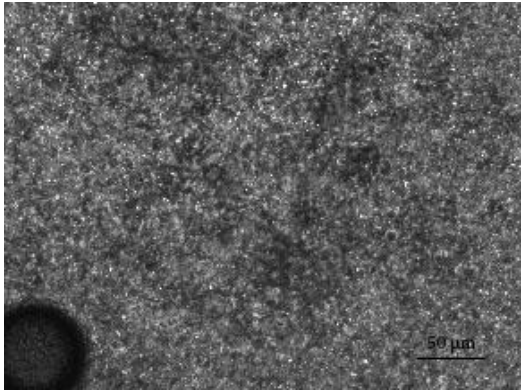


FIGURE 13: RESULTS OF ASCORBIC ACID ENHANCED DIFFERENTIATION PROCEDURE

5.1.3 Modified Serum Level Results

Below are images of cells grown on tissue culture plastic with the standard and modified serum protocols. All plates from day 15 to 30 stained positive for deposits of proteoglycans and appeared similar to the original validation of this protocol, but large deposits of proteoglycans first appeared in the modified serum group. This modified protocol group also showed faster changes in morphology and the cells were more granular in appearance.

Standard serum protocol (20x)	Modified serum protocol (20x)	
		<p>Day 15</p>

 <p>50 μm</p>	 <p>50 μm</p>	<p>Day 18</p>
 <p>50 μm</p>	 <p>50 μm</p>	<p>Day 21</p>
 <p>50 μm</p>	 <p>50 μm</p>	<p>Day 24</p>

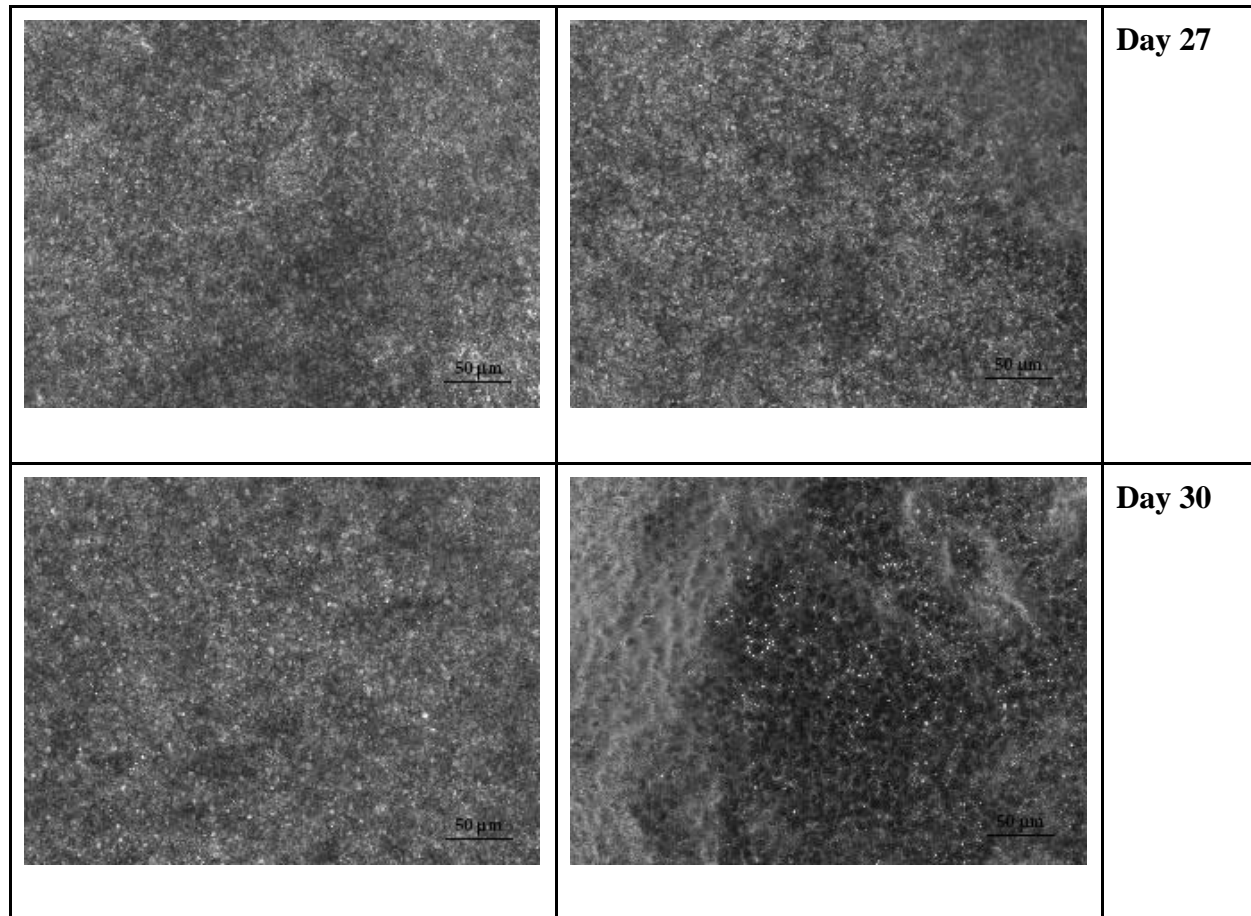


FIGURE 14: RESULTS OF MODIFIED SERUM LEVEL ON ATDC5 DIFFERENTIATION

5.1.4 Cellular Distribution Results

The results of the cellular distribution experiment can be seen below. Solutions at each time point shown in the figure formed a solid gel, so damage to the cross links in the hydrogel appeared to be minimal. The low focal plane was determined using the 0 minute group at the level where cells could first be seen while moving from the bottom of the plate through the gel. Images of all wells were taken at this same focal plane and cells could still be seen in the 30 minute wells. The high focal plane was determined using the 30 minute wells by moving the focal plane down through the gel. All time points were imaged and compared at this upper focal plane. Less cells were in focus in the 20, 10, and 0 minute wells, confirming a wider distribution of cells in the 30 minute wells. Given this wider distribution and the fact that it still made an intact hydrogel, scaffolds were seeded with cells in a gel allowed to remain at 25 degrees Celsius for 30 minutes.

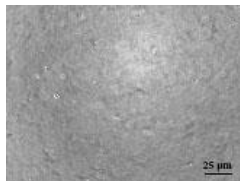
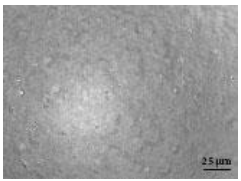
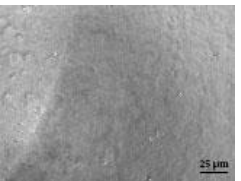
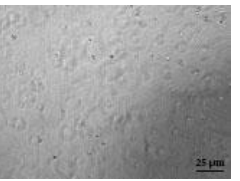
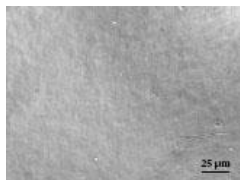
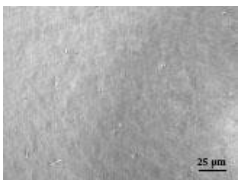
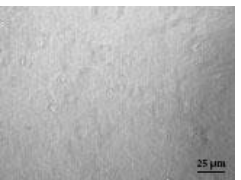
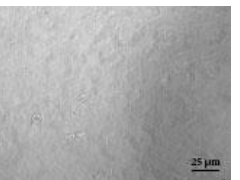
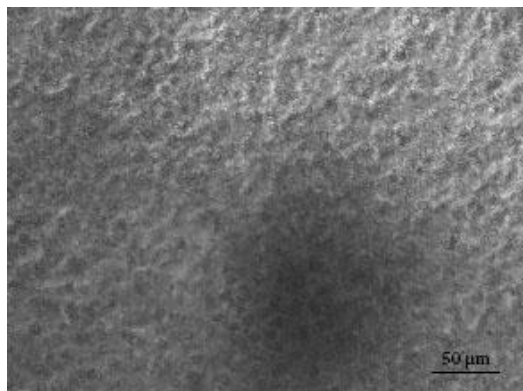
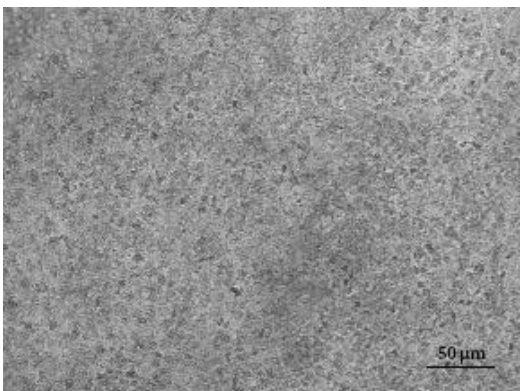
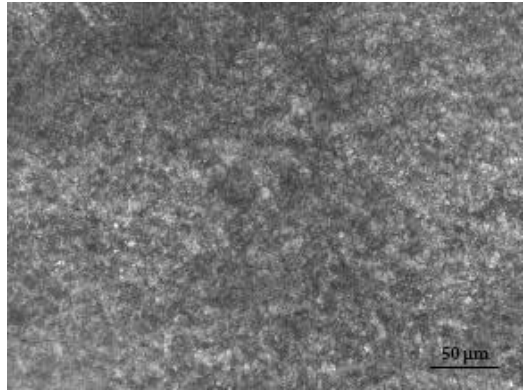
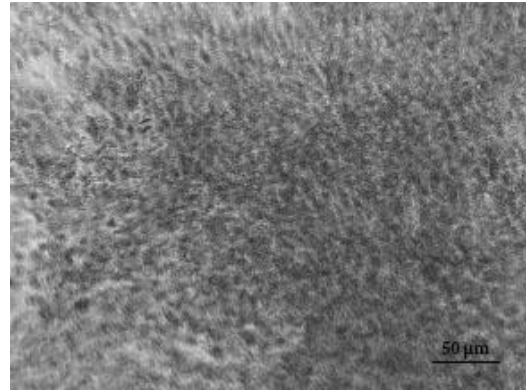
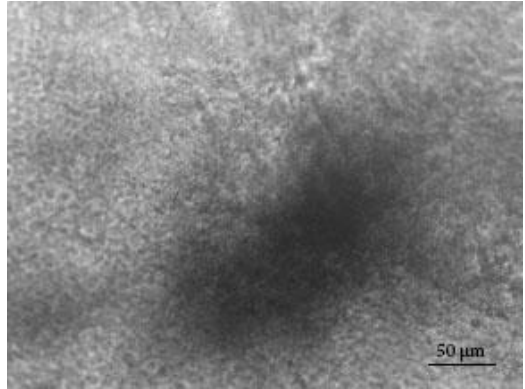
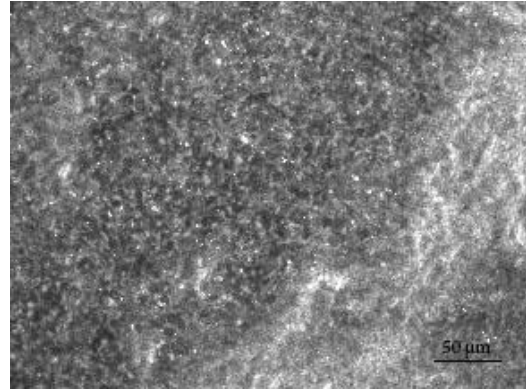
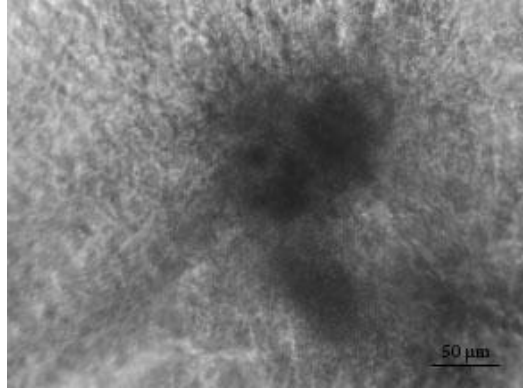
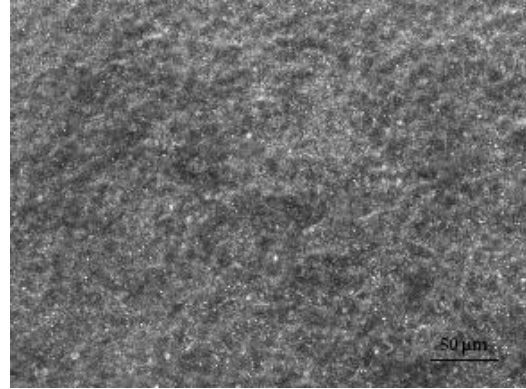
	0 minutes	10 minutes	20 minutes	30 minutes
High focal plane (20x)				
Low focal plane (20x)				

FIGURE 15: RESULTS OF CELLULAR DISTRIBUTION EXPERIMENT WITH 25µM SCALE BARS

5.1.5 ATDC5 Differentiation in Collagen Hydrogel Results

The results of the ATDC5 differentiation in the collagen hydrogel can be seen below. Cells were fixed and stained on days 15, 18, 21, 24, 27, and 30. Both groups of cells, those grown in the hydrogel and on tissue culture plastic, displayed patches of deposited proteoglycans when stained with Alcian blue. These deposits of proteoglycans indicate differentiation into chondrocytes. This is the final indication of chondrogenesis. These patches grew in size and number from day 15 to 30 along with an increase in how granular the cells appeared. Cells grown in the hydrogel showed larger deposits of proteoglycans which appeared earlier over the course of the experiment.

Collagen hydrogel (20x)	Tissue culture plastic (20x)	
		Day 15

 <p>50 μm</p>	 <p>50 μm</p>	<p>Day 18</p>
 <p>50 μm</p>	 <p>50 μm</p>	<p>Day 21</p>
 <p>50 μm</p>	 <p>50 μm</p>	<p>Day 24</p>

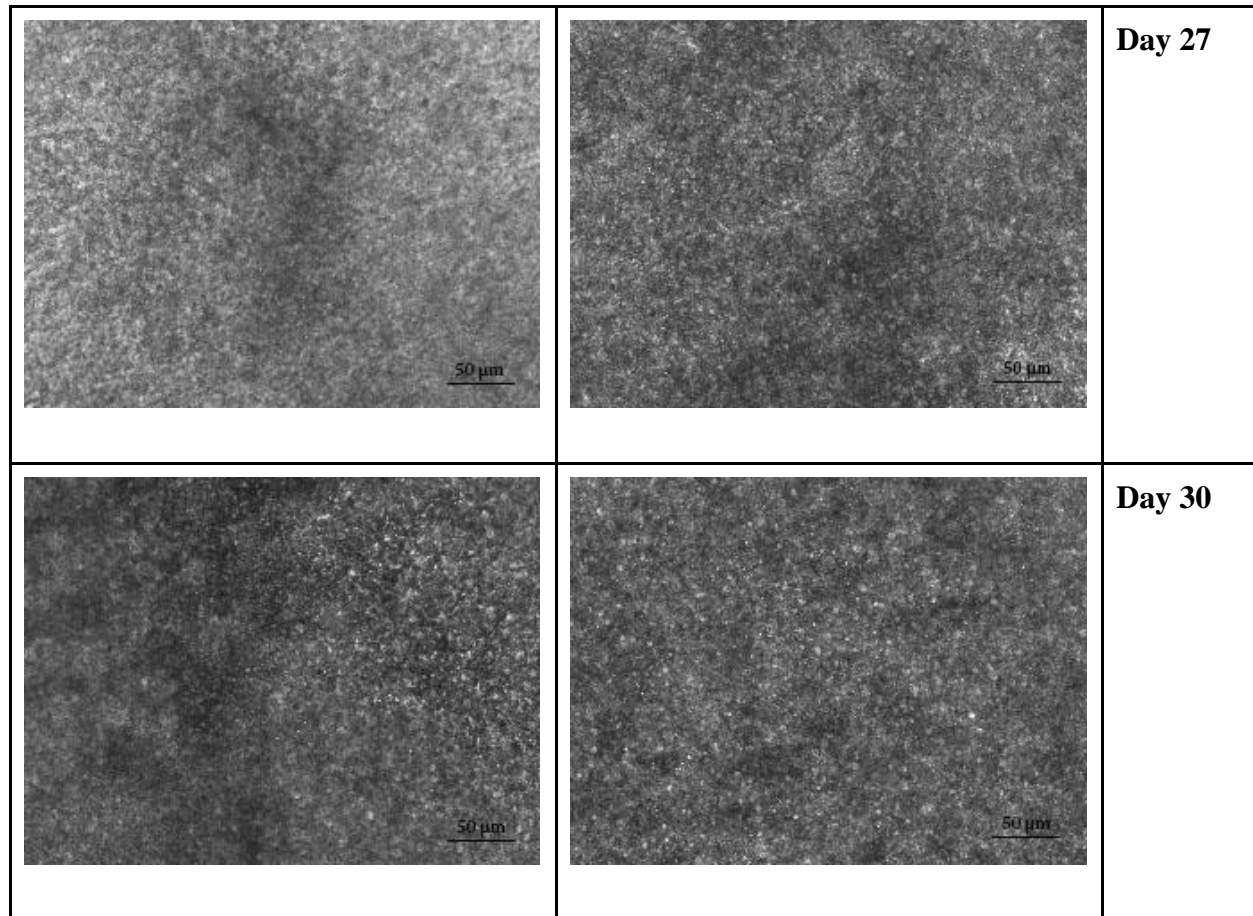


FIGURE 16: RESULTS OF ATDC5 DIFFERENTIATION WITHIN COLLAGEN HYDROGEL

5.2 PLA Degradation Results

TABLE 8: DEGRADATION RESULTS

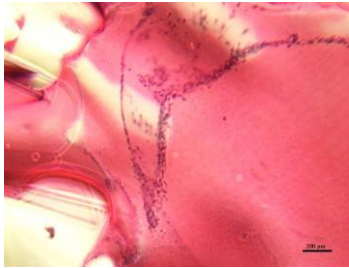
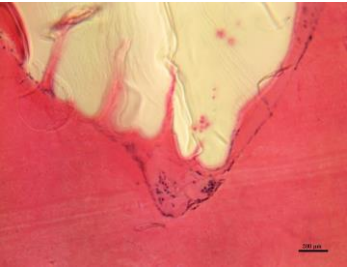
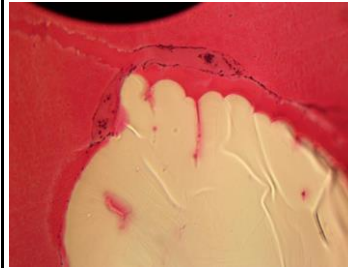
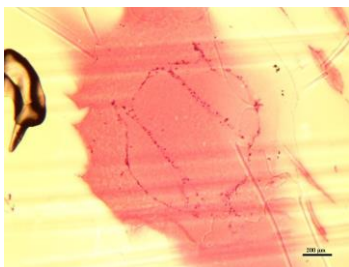
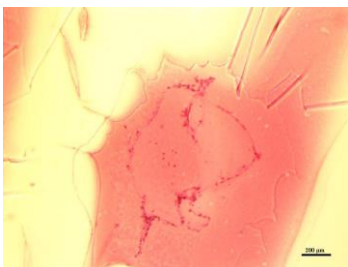
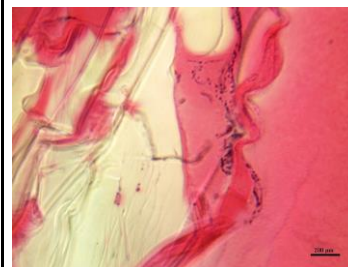
Time in solution (days)	1	7	14	21	28
Initial Weight (g)	0.340	0.343	0.345	0.346	0.338
Final Weight (g)	.343	.346	.347	.348	.339

The PLA filament compatible with the MakerBot® 3D printer has a slow degradation rate compared to that of the compatible PVA filament. Five whole scaffolds were printed in PLA and placed in distilled water at 37°C for a range of days, ranging from 1 day in water to 28 days, and were then dried, weighed, examined, and compared under a microscope. The weights of the samples were all within one-tenth of a gram of one another and did not show the change in

weight we were expecting. This is most likely because the five individual prints were not identical in weight to one another and the polymer degradation is negligible compared to the printing precision. The defects caused by printing also made it difficult to tell how each scaffold varied from one to the other. PLA also undergoes bulk degradation rather than surface degradation so the edges are not the first place degradation is necessarily visible. Given the accuracy of the scale used, quantifiable results were not able to be obtained for the degradation of the MakerBot® PLA over the timeframe of the ATDC5 differentiation.

5.3 Histology Results

The results of the H&E and the Phalloidin/DAPI staining are shown below in Figures 18 and 19, respectively. For the H&E staining, representative images were obtained for both single and modular scaffolds for the Original or Modified culture protocol. The modular scaffolds were split into their base pieces and processed separately. The scaffolds with the large central pore on each side are labeled “Middle” and the scaffolds with the smaller pores on each side are labeled “Outer.” Each image is from a slice that is from the outer (0-1.5 mm), middle (1.5-3.0 mm), or inner (3.0-4.5 mm) section of the scaffold.

	Outer (0-1.5mm)	Middle (1.5-3.0mm)	Inner (3.0-4.5mm)
Modified Protocol Middle (A)			
Modified Protocol Outer (B)			

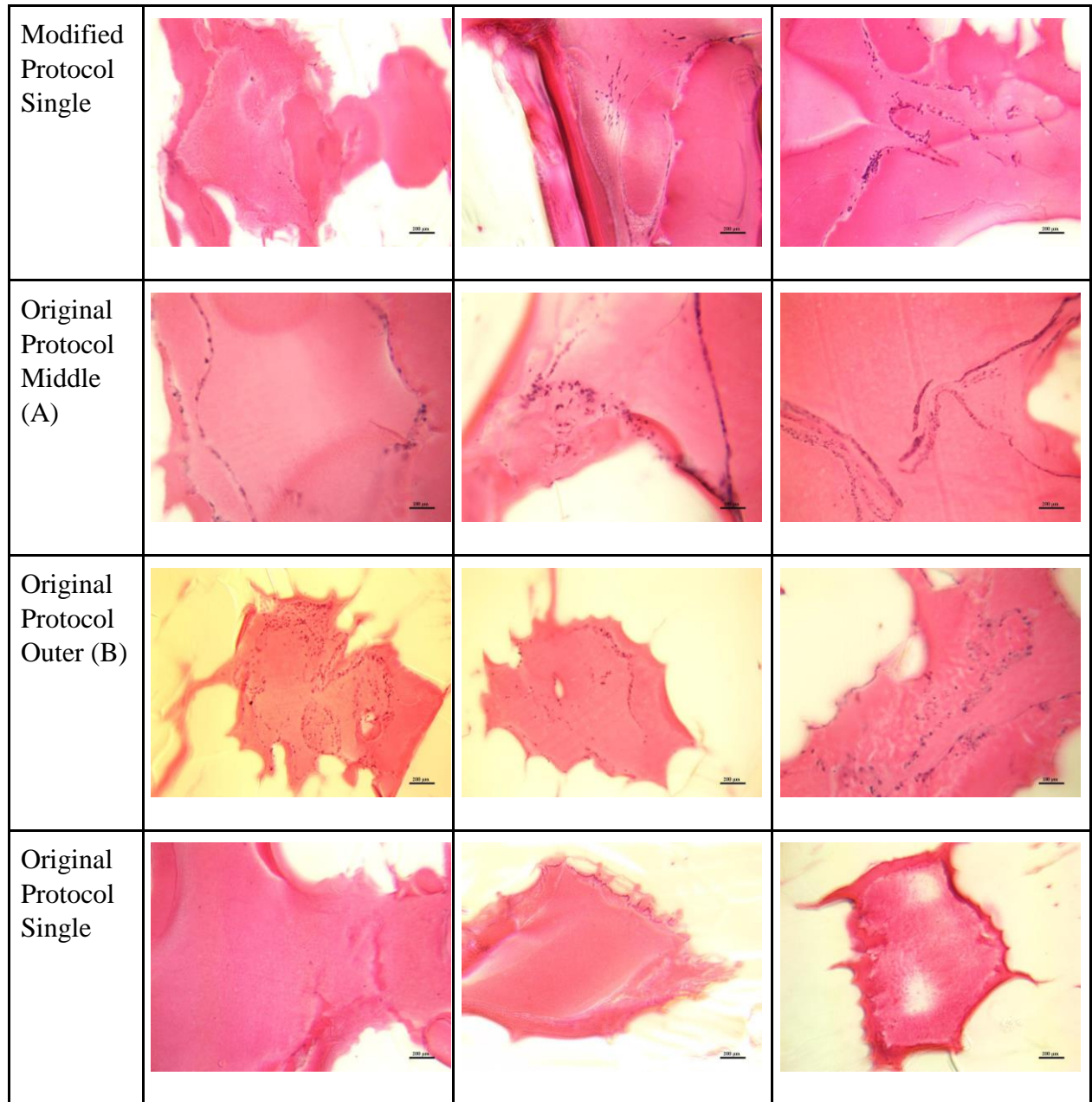


FIGURE 17: H&E STAINING OF 5UM SCAFFOLD SLICES AT DIFFERENT DEPTHS

Sections are all at 10x magnification with the exception of the Original Protocol Middle Scaffold Outer and Middle sections, and the Original Protocol Outer Scaffold Inner section.

For the Phalloidin/DAPI fluorescent staining, sections from a Modified Protocol Middle and Single scaffold were stained.

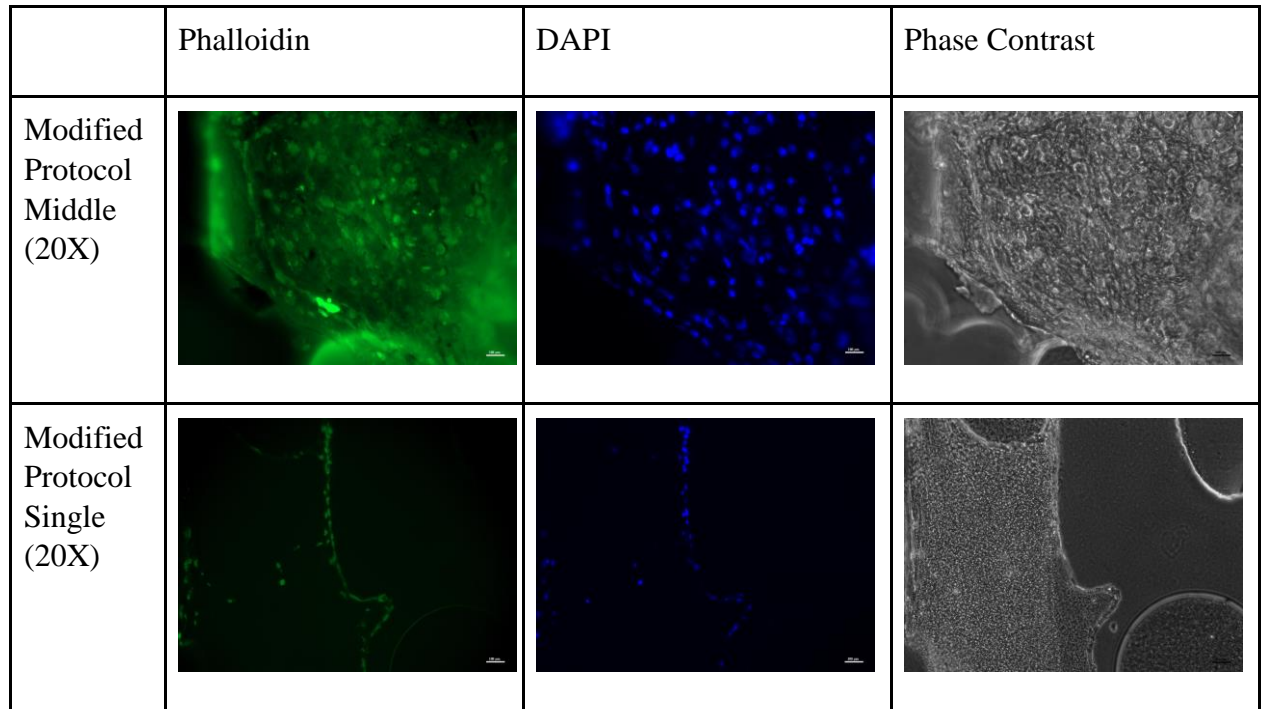


FIGURE 18: PHALLOIDIN/DAPI STAINING OF SCAFFOLDS. LEFT-RIGHT: PHALLOIDIN STAIN, DAPI STAIN, PHASE CONTRAST IMAGE

5.4 Modular Scaffold Results

Staining the inner face of the modular scaffolds revealed proteoglycan deposits in the modified group at day 15 and the normal group at day 22, confirming the ability for the fractal geometry to allow proper nutrient penetration. These stained deposits can be compared against a negative control where the entirety of the Alcian blue stain washes out. The significance of these proteoglycan deposits as a viability marker confirm the scaffold design can allow cells to proliferate and differentiate at a depth of 3mm.

Chondrogenesis at day 15 in modified protocol (4x)	Chondrogenesis at day 22 in original protocol (4x)
----------------------------------------------------	----------------------------------------------------

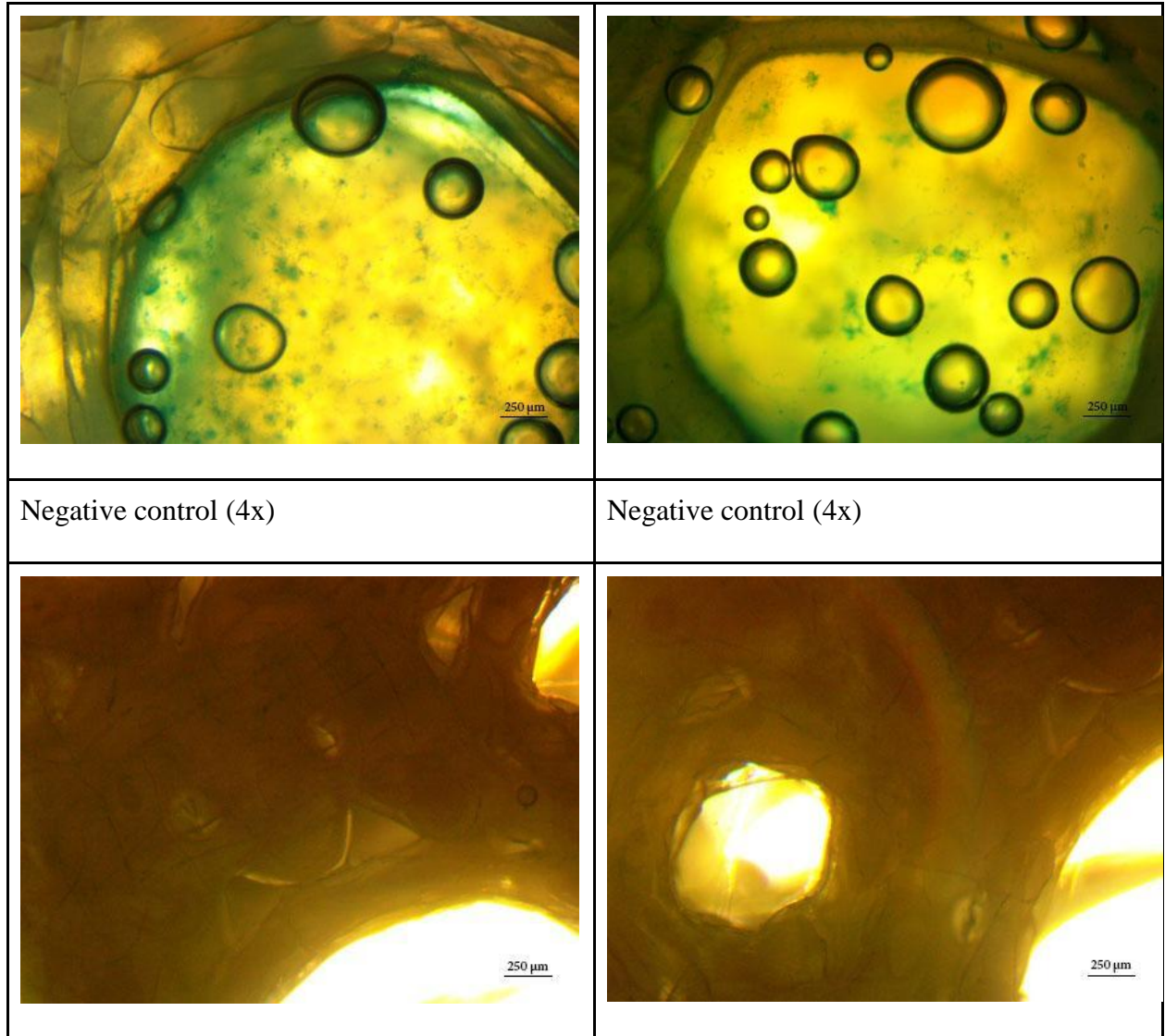


FIGURE 19: SECTIONED AND STAINED MODULAR SCAFFOLD COMPARED TO A NEGATIVE CONTROL

Figure 19: Sectioned and stained modular scaffold compared to a negative control

6. Discussion

The data presented in **Figure 17** shows cell staining at several scaffold depths for different scaffold designs and tissue culture protocols. Cells were present at all depths for each scaffold and protocol tested, though the Original Protocol Single scaffolds had very few cells. These results imply that the scaffolds were able to successfully support cells at depths up to 3mm. Interestingly, the larger, modular scaffolds had a much greater amount of cells at greater depths than either single scaffolds, implying that the more complex geometry of the modular scaffolds had an effect in increasing cell proliferation. Additionally, the cells typically appear in

curving “sheets” several cell-lengths thick, which implies an organized structure. The Phalloidin/DAPI staining in **Figure 18** agrees with this interpretation, as it shows that the cellular actin, which serves as the cytoskeleton and gives cells their shape, was organized into sheets coaxial to the hydrogel-PLA barrier similar to that seen in the H&E staining.

While the cells appear too organized and proliferating in the scaffolds, the team noticed an interesting trend with regards to the localization of the cell sheets. In almost all samples, cells appeared to localize to the periphery of the hydrogel, closest to the PLA structures (this is apparent in figures **17** and **18**). However, the team also noticed that large “folded planes” of cells were visible on test slides outside of the scaffold structures (examples shown in **Appendix G**). The team believes that these disembodied planes of cells were initially located within the scaffold, but were sheared off during microtome sectioning. Even with acetone treatment, the PLA scaffold is much stiffer than the cell-laden hydrogel, and the resulting heterogeneity of stress during sectioning could deform the hydrogel and move it out of plane. During each cut, the out-of-plane cells/hydrogel are transplanted from inside the scaffold to the surrounding hydrophilic paraffin wax, and are then immobilized once the section is glued to a test slide.

The team also conducted Alcian Blue staining on whole scaffolds to look for proteoglycan deposits (shown in **Figure 19**). Proteoglycan deposits are a sign of chondrogenesis, so increased deposits implies that the cells survived long enough to differentiate (21-28 days). The adapted modified protocol used to seed and culture the scaffolds showed more chondrogenesis given the results of the Alcian blue staining. This is due in part to the seeding of prechondrocytes instead of untreated ATDC5 cells as well as the modified serum levels. The preliminary cell experiments showed these lowered serum levels result in faster differentiation and this was demonstrated again in the tissue engineered constructs. Higher levels of these proteoglycan deposits are present towards the surface of the scaffold. This is due to the slight degradation of the PLA over the course of culturing the tissue engineered construct. This resulted in an increase in nutrient perfusion, showing the effect the biomorphic scaffold had on the ATDC5 cells grown within it.

6.2 Economics

The economics of this technology are within the means of many small labs and startup companies. Many of the labs and corporations haven’t explored using 3D printing to create cell

scaffolds due to the high costs of rapid prototyping machines. However, given that a low cost commodity 3D printer can be used to create biomorphic scaffolds like the ones in the project, the cost of entry has been significantly lowered for the ability to create cell scaffolds for this type of research.

6.3 Environmental impact

The environmental impact of this technology is fairly low overall. The material used for printing is fully biodegradable, and the manufacturing process used to create the scaffolds resulted in a minimal amount of this material that needed to be discarded. The tissue engineering and cell culture required to create tissue engineered constructs from these biomorphic scaffolds contributed more to the environmental impact of this technology than manufacturing the scaffolds. This is due to the large amount of sterile single use products that need to be used. This includes tissue culture plates, bottles, serological pipettes, and micropipette tips used to culture cells and tissue as well as seed the scaffolds. Scaling up this process and fairly simple and could result in lessening the environmental impact. Commodity 3D printers and available for low costs and further improvements could be made in the manufacturing process to lessen discarded material. Scaling up the tissue culture could involve automated processes, but a dedicated professional would still be required to seed scaffolds with cells.

6.4 Societal influence

This technology, if commercialized, would have a significant impact on society. This proof of concept could be further developed to revolutionize the way meniscal tears and avascular cartilage damage is treated. Not only could this method of scaffold creation be used to create a fractal inspired scaffold to grow a tissue engineered construct in the shape of the full meniscus, but a patient's wound site could be imaged and a fractal inspired cell scaffold could be created that conforms specifically to this wound site. A scaffold could be implanted to prevent scarring while another is cultured with cells before replacing the preliminary scaffold, eventually fully replacing the patient's damaged or missing tissue. However this project is only a proof of concept and further testing needs to be conducted. This could include growing larger tissue as well as implanting these tissue engineered constructs into living systems.

6.5 Political ramifications

The only political concerns of this technology would be the use of certain cell lines. The controversy of using embryonic stem cells could be avoided by using induced pluripotent stem cells produced from the patients' native cells. If the politics of embryonic stem cell lines can be avoided, and given the low cost of manufacturing these scaffolds, this technology has the potential to improve global health care, including developing countries.

6.6 Ethical concerns

There are many ethical concerns given the implantation of living cells as a form of therapy. There is the potential of immortalized cell lines to continue proliferating and forming cancer in a patient's body. Furthermore, implanting living cells into the body of patients could lead to an infection caused by an undiscovered virus or other form of contamination in the manufacturing and tissue engineering processes.

6.7 Health and safety issues

There are no immediate health and safety issues in terms of this preliminary research. If this technology is further pursued and scaled up for use commercially, FDA and ISO standards will need to be met and adhered to. Potentially issues which will need to be explored include how the laboratory differentiated cells will incorporate into the native tissue and how the native cells will interact with the scaffold. The healing time of implantation procedures will need to be taken into consideration as well as avoiding scar formation around the tissue engineered construct. Finally, interactions with the implanted PLA and the native tissue will need to be explored and addressed as necessary.

6.8 Manufacturability

The manufacturability of these scaffolds is fairly straight forward. They can be created with an unmodified commodity 3D printer, but simple modifications could be made to increase resolution and improve the surface area to volume ratio. The manufacturing process could be scaled up given the relatively cheap cost of these printers. The tissue engineering and cell culture can be scaled up as well with the inclusion of automated processes, but there still needs to be a dedicated professional to seed the scaffolds with cells.

6.9 Sustainability

This technology and manufacturing process have a low economic and environmental impact, leading to this process being highly sustainable. Overall this manufacturing process required a small amount of financial capital to begin and used limited material resources. The most expensive aspect of this research includes the cost of sterile single use lab equipment and culturing media used for growing cells and seeding scaffolds. Overall, this process is sustainable for small research labs as well as startup companies to continue given the results and clinical significance.

7 Final Design

The final scaffold design used for this project was a second level recursion cylindrical Menger Sponge. For ease of processing and cellular visualization the scaffold was broken into three modular sections; an identical top and bottom section and a middle section. Each of these scaffold sections were 9mm x 9mm x 3mm while the second level of pores had a diameter of 1mm and the central pores had a diameter of 3mm. The central pores located on the side of the middle section of scaffold had a diameter 2.5 mm. The second level of recursion of the final design allowed for nutrient penetration to the core of the scaffold and the reduction of cell necrosis. This design was also less computationally demanding and could be processed with the resources available to the group.

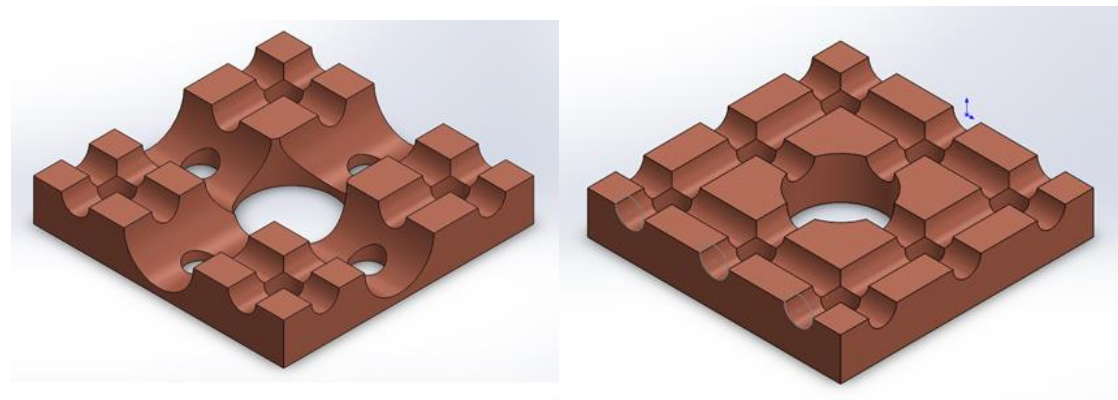


FIGURE 20: CAD MODEL OF MODULAR SCAFFOLD SECTIONS OF 2ND LEVEL RECURSION CYLINDRICAL Menger SPONGE - CROSS SECTIONED VIEW

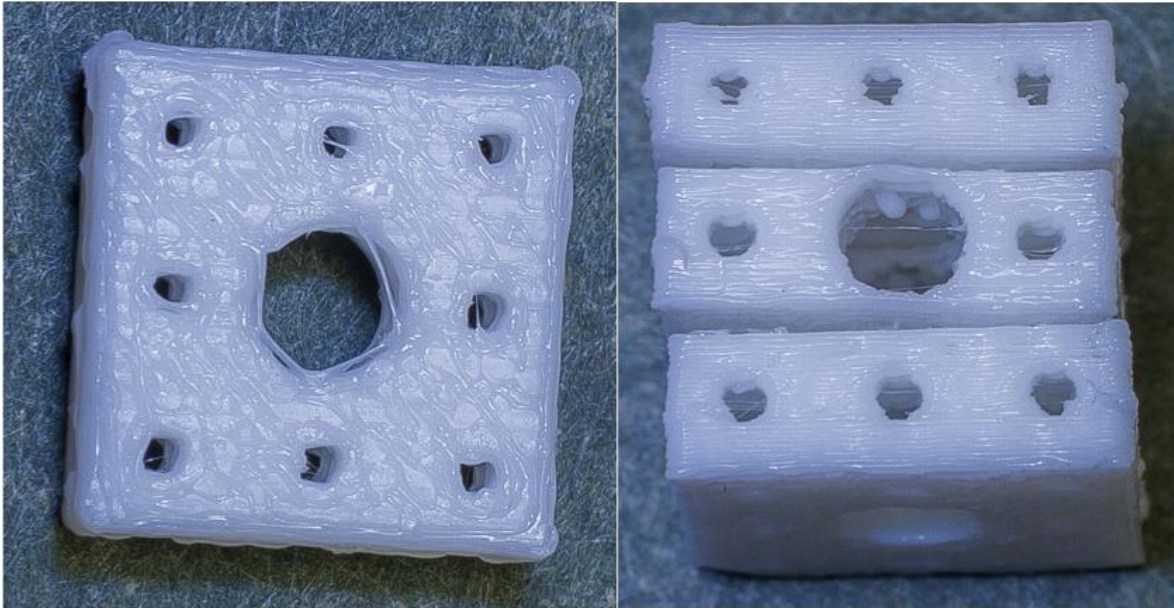


FIGURE 21: 3D PRINTED PLA MODULAR SCAFFOLD SECTIONS OF SECOND LEVEL RECURSION CYLINDRICAL MENGER SPONGE (LEFT TO RIGHT: TOP DOWN VIEW, STACKED SIDE VIEW)

A current limitation of thick tissue culture is the necrosis of cells within the center of the culture over time. Typical thick tissue engineering deals with tissue growth by the plating of cells in a two dimensional culture. These cells are cultured in complete media and allowed to grow. As the cells continue to grow in the culture plates they begin grow atop one another and this prevents nutrients from reaching the cells at the bottom of the tissue, leading to cell necrosis. This cell necrosis can occur in tissue deeper than 1mm (Rajagopalan & Robb 2006) and is a great limitation for current thick tissue culture

Biodegradable scaffolds show promise in preventing cell necrosis by allowing increased nutrient penetration of the thick tissue culture due to the 3D structure of the scaffold. As the scaffold degrades as the cells begin to grow and proliferate this allows nutrients to penetrate into the core of the scaffold and reach the cells within, reducing cell necrosis throughout the scaffold. Our design focused on the use of fractals, such as a Menger Sponge fractal, to increase the surface area to volume ratio of our biodegradable scaffold. An increased surface area allows for greater cell proliferation and an increased degradation rate of the scaffold, as well as an increased volume of nutrients that can be delivered to the cells.

Our scaffold design allowed cells to survive long enough to differentiate into thick tissue. This was visualized via cellular expression of proteoglycans. The edges and surfaces of the

scaffold seemed to improve localized cell proliferation while cells were seen to conform to the curves of the scaffold. This conformation was seen by the presence of actin filaments, a major cytoskeletal component, during histology testing. The visualization of proteoglycans and the conformation and localization of cells to the surfaces and curves of the scaffold implies that there was nutrient flow due to the degradation of the scaffold. This increased nutrient flow showcases the advantages of using a three dimensional, biodegradable scaffold for thick tissue engineering and the reduction of overall cell necrosis.

While our scaffold design showed improved nutrient penetration to the cells within the scaffold there are some limitations to the scaffold design. Our final scaffold design was a second level recursion cylindrical Menger Sponge that was broken into three modular sections for ease of processing and cell visualization. This second level of recursion of the fractal allowed for an adequate surface area to volume ratio but an increased level of recursion in the scaffold, such as a third or fourth level of recursion, would allow for an increased ratio and therefore an increase in nutrient flow. Our ability to generate an increase in the recursion level of our scaffold design is limited to computational overhead that the group has access to.

All scaffolds were printed using a MakerBot® Replicator 2, where the print settings had been modified to increase the resolution of the scaffold. Without modifying the hardware of the printer the group was able to print large quantities of the scaffold. The Replicator 2 is a commercially available printer that costs two thousand dollars, a large decrease in price compared to other industrial printers that can easily cost upwards of ten thousand dollars. The PLA used to print the scaffolds came in the form of a 1kg spool and cost eighty dollars. Based off the amount of scaffold sections the group was able to print using a 1kg spool of PLA a single printer could print hundreds of scaffold sections at a pennies per scaffold section. Manufacturing these scaffolds on a large scale can be economically feasible if this project was to develop.

The success of this scaffold design shows that our scaffold device is a novel method to culture thick tissue. This project also has shown that 3D printing allows for the creation of complex geometries that can be used to increase the surface area to volume ratio, something that is shown to be vital for nutrient penetration and delivery to cells in thick tissue culture. That these scaffolds were created on a commercially available printer shows that it is possible to print these complex geometries on most any type of commercially available printer. These printers can

potentially be modified to increase the resolution of any future printed scaffolds and as commercially available printers are much cheaper to purchase than industrial 3D printers, this makes these printers ideal for use in any further research into thick tissue engineering.

8 - Conclusions and Recommendations

This project focused on engineering cartilaginous tissue in 3D printed PLA scaffolds. The following section outlines the conclusions drawn from our results, recommendations for future improvements, and the impact on the thick tissue engineering.

8.1 - Objectives

The main objective of this project is developing a novel method for thick tissue culture that creates a viable environment for cell proliferation and differentiation into cartilaginous tissue using a biodegradable scaffold that is printed using a commodity 3D printer. The results derived from this project show the objective has been met: the scaffolds' design influenced the cell's behavior. The following highlights some of the ways in which the project's objectives were met.

The scaffold itself was created to provide a high surface area to volume ratio in order to provide nutrients to the center of the thick tissue, which was hypothesized to prevent necrosis. In order to test the viability of cells in the center of the scaffold, the modular scaffold design was created so cells that were located in the thick part of the scaffold could be analyzed. Imaging and staining cells within the modular thick scaffolds show the cells' structure mimic that of cartilage and also proves the viability of the cells as the amount of proteoglycans present in the scaffolds increased over time, proving presence of cartilaginous tissue and that the cells were viable up to 21 days when these secretions are produced. The location and geometry of cells and cytoskeleton with relation to the scaffold walls showed the scaffolds influence over the cells. For example, the density of proteoglycan deposits near the walls of the scaffold pores relative to the density of the inner portion of the pores was much greater. Images of the cells also showed alignment along the scaffold walls.

8.2 - Future Improvements

While this project achieved its overarching objective, there are many avenues for improvement due to the limited time constraints and available resources. Some areas for future

improvement include providing greater computing power, better printer resolution, and creating a customizable polymer as well as engineering whole cartilaginous tissues.

Fractal CAD models, both open source and custom made, often require a lot of computing power to manipulate because of their high level of detail. This intricate detail made the CAD software available throughout our project run very slowly and often crash. Access to greater computing power would allow greater fractal recursion levels, the creation of more complex gross geometries, such as a meniscus, out of the modular scaffold “building blocks,” and making a more intricate way of connecting the modular blocks together, which were both limited due to insufficient computing power.

Manufacturing the scaffolds using the Replicator2 3D printer with the default settings does not allow for a high enough resolution to print the small details of the scaffolds. The resolution can be slightly modified two ways: the ReplicatorG software itself can be changed since it is an open source program or the printer hardware can be modified. The ReplicatorG software allows the user to modify the feeds and speeds of the extruder as well as the level of the build plate while the physical nozzles of the printers can be changed for ones with different diameters. Even with these possible modifications to improve printer resolution, the fractals with higher recursion levels could not be printed.

PLA, the biodegradable polymer that is used in these scaffolds, is the commercially available filament sold from the MakerBot®. Different grades of PLA will have different degradation rates depending on the molecular weights of the filament. A custom polymer having a molecular weight that allows it to degrade at a rate close to that of the rate of cell proliferation would cause better nutrient flow throughout the scaffold. The two biodegradable polymers that have filaments compatible with 3D printing, PLA and PVA both experience bulk degradation. Bulk degradation occurs uniformly throughout the entire scaffold. Surface degradation, where the scaffold degrades first from the edges and pores of the scaffold, would also allow for better nutrient flow.

The next step in further developing this project is to begin creating differing gross geometries; for example, the knee meniscus, out of the smaller “building block” scaffolds developed in this project. Since some of the cartilaginous tissue in the body is thicker than that which we experimented with, viability testing would be necessary to make sure there is not a

necrotic core. Mechanical testing of the tissue would also be necessary as the scaffold degrades to ensure the engineered tissue is mechanically similar to the natural tissue. Further testing and clinical trials would also have to be done using human cells, either allogeneic or autologous chondrocytes, prior to clinical use.

8.3 - Clinical Importance

This method for engineering thick tissues has the potential to make an impact on the industry standard because of the accessibility of the technology and resources necessary to replicate this work in a clinical setting. Hypothetically, if the steps in the *Previous Works* section above, as well as clinical trials were carried out and proven successful, providing more effective surgery for cartilage damage, such as the meniscus, would be possible. A doctor could take an MRI image of a damaged tissue and have a scaffold replicated and 3D printed in the gross structure of a patient's tissue. The PLA scaffold would have an internal configuration of different scaled Menger Sponge scaffold blocks, which, when seeded with either allogeneic or autologous chondrocytes and grown into the tissue, would provide mechanical properties similar to a healthy tissue. The technology discussed in this paper is still far from being used in a clinical setting, as discussed in the *Previous Works* section above, but the potential for clinical improvement is great.

References

- Alblas, J., Dhert, W. J. A., Fedorovich, N. E., Hennink, W. E., & Oner, F. C. (2011). Organ printing: the future of bone regeneration? *Trends in Biotechnology*, 29(12), 601-606.
- ATDC5. from http://hpacultures.org.uk/products/celllines/generalcell/detail.jsp?refId=99072806&collection=ecacc_gc
- Binder, K. W. (2011). *In Situ Bioprinting of the Skin*. (Doctor of Philosophy), Wake Forest University Graduate School of Arts and Sciences.
- Boland, T., Cui, X., Damon, B., & Xu, T. (2006). Application of inkjet printing to tissue engineering. *Biotechnology Journal*, 1(9), 910-917. doi: DOI 10.1002/biot.200600081
- Boland, T., Forgacs, G., Markwald, R. R., Mironov, V., & Trusk, T. (2003). Organ printing: computer-aided jet-based 3D tissue engineering. *Trends in Biotechnology*, 21(4), 157-161.
- Bradshaw, S., Bowyer, A., & Haufe, P. (2010). The Intellectual Property Implications of Low-Cost 3D Printing. *ScriptEd*, 7(1), 5-31.
- C3H/10T1/2. from <http://www.atcc.org/products/all/CCL-226.aspx>
- Chamberlain, G., Fox, J., Ashton, B., & Middleton, J. (2007). Concise Review: Mesenchymal Stem Cells: Their Phenotype, Differentiation Capacity, Immunological Features, and Potential for Homing *Stem Cells*.
- Chichkov, B., Gruene, M., Koch, L., & Unger, C. (2013). Laser Assisted Cell Printing. *Current Pharmaceutical Biotechnology*, 14(1), 91-97.
- David, J. (1974). Ariadne Column. *New Scientist*.
- Denker, A., Haas, A., Nicoll, S., & Tuan, R. (1999). Chondrogenic Differentiation of Murine C3H10T1/2 Multipotential Mesenchymal Cells: I. Stimulation by Bone Morphogenetic Protein-2 in High-Density Micromass Cultures *Differentiation*, 64.
- Fan, J., Varshney, R., Ren, L., Cai, D., & Wang, D.-a. (2009). Synovium-Derived Mesenchymal Stem Cells: A New Cell Source for Musculoskeletal Regeneration *Tissue Engineering*, 15.
- Fox, A.J.S., *et al.*, (2011). The Basic Science of Human Knee Menisci: Structure, Composition, and Function (pp.343-8) *Sporth Health: A Multidisciplinary Approach. Vol 4*.
- Gozuacik, D., Karakas, H. E., Koc, B., Kucukgui, C., & Ozler, B. (2013). 3D Hybrid Bioprinting of Macrovascular Structures. *Procedia Engineering*, 59, 183-192.
- Haas, A., & Tuan, R. (1999). Chondrogenic Differentiation of Murine C3H10T1/2 Multipotential Mesenchymal Cells: II. Stimulation by Bone Morphogenetic Protein-2 Requires Modulation of N-Cadherin Expression and Function *Differentiation*, 64.

- Hall, B. (2005). *Cartilage Bones and Cartilage: Developmental and Evolutionary Skeletal Biology* (pp. 16).
- Hattori, K., Takakura, Y., Ishimura, M., Uematsa, K., Ikeuch, K. (2004). Quantitative arthroscopic ultrasound evaluation of living human cartilage (Vol. 19, pp. 213-216). *Clinical Biomechanics*.
- Hsu, Y. H., I. G. Turner, and A. W. Miles. “Fabrication of Porous Bioceramics with Porosity Gradients SIMilar to the Bimodal Structure of Cortical and Cancellous Bone.” [In English]. *J Master Sci Mater Med* 18, no 12 (Dec 2007): 2251-6
- Hunter, C. (2011). Fibrocartilage Tissue Engineering. In J. Burdick & R. Mauck (Eds.), *Biomaterials for Tissue Engineering Applications*.
- Johns, D. E., & Athanasiou, K. A. (2008). Growth Factor Effects on Costal Chondrocytes for Tissue Engineering Fibrocartilage. *Cell Tissue Res*.
- Katagiri, H., Muneta, T., Tsuji, K., Horie, M., Koga, H., Ozeki, N., . . . Sekiya, I. (2013). Transplantation of Aggregates of Synovial Mesenchymal Stem Cells Regenerates Meniscus more Effectively in a Rat Massive Meniscal Defect. *Biochemical and Biophysical Research Communications*, 435.
- Ko, H., Milthorpe, B., & McFarland, C. (2007). ENGINEERING THICK TISSUES – THE VASCULARISATION PROBLEM. *European Cells and Materials*, 14, 1-19.
- Liu, Z.-J., Zhuge, Y., & Velazquez, O. (2009). Trafficking and Differentiation of Mesenchymal Stem Cells. *Journal of Cellular Biochemistry*.
- Manoharan, R. (2004). Side-viewing fiberoptic catheter for biospectroscopy applications (Vol. 19, pp. 15-20). *Lasers in Medical Science*.
- Martin, I., Obradovic, B., Freed, L. E., & Vunjak-Novakovic, G. (1999). Method for Quantitative Analysis of Glycosaminoglycan Distribution in Cultured Natural and Engineered Cartilage. *Annals of Biomedical Engineering*, 27, 656-662.
- Mo, X.-t., Guo, S.-C., Xie, H.-q., Deng, L., Zhi, W., & Xiang, Z. (2009). Variations in the Ratios of Co-Cultured Mesenchymal Stem Cells and Chondrocytes Regulate the Expression of Cartilaginous and Osseous Phenotype in Alginate Constructs. *Bone*.
- Mow, V., Gu, W. Y., Chen, F. H., Vunjak-Novakovic, G., & Goldstein, S. (2005). *Basic Orthopaedic Biomechanics and Mechano-Biology* (3rd ed.).
- Ohno, T., Hashimoto, N., Mitsui, K., Nishimura, H., & Hagiwara, H. (2012). Iron Overload Inhibits Calcification and Differentiation of ATDC5 Cells. *J. Biochem*.
- Ozbolat, I. T., & Yu, Y. (2013). Bioprinting Toward Organ Fabrication: Challenges and Future Trends. *Biomedical Engineer, IEEE transactions*, 691-699. doi: 10.1109/TBME.2013.2243912

- Park, K., Min, B.-H., Han, D. K., & Hasty, K. (2006). Quantitative Analysis of Temporal and Spatial Variations of Chondrocyte Behavior in Engineered Cartilage during Long-Term Culture. *Annals of Biomedical Engineering*, 35(3), 418-428.
- Pazzano, D. (1999). The Characterization OF Chondrogenesis in a Perfusion Bioreactor System: Effects OF Media pH and Fluid Flow on Matrix Assembly. Worcester Polytechnic Institute.
- Rajagopalan, S., & Robb, R. A. (2006). *Schwarz meets schwann: Design and fabrication of biomorphic and durataxic tissue engineering scaffolds*. *Medical Image Analysis*, 10, 693.
- Raum, K. (2004). *Ultrasonic Nondestructive Evaluation: Engineering and Biological Material Characterization*: CRC Press LLC.
- Shukunami, C., Ishizeki, K., Atsumi, T., Ohta, Y., Suzuki, F., & Hiraki, Y. (1997). Cellular Hypertrophy and Calcification of Embryonal Carcinoma-Derived Chondrogenic Cell Line ATDC5 In Vitro. *Journal of Bone and Mineral Research*, 12(8).
- Shukunami, C., Shigeno, C., Atsumi, T., Ishizeki, K., Suzuki, F., & Hiraki, Y. (1996). Chondrogenic Differentiation of Clonal Mouse Embryonic Cell Line ATDC5 In Vitro: Differentiation-dependent Gene Expression of Parathyroid Hormone (PTH)/PTH-related Peptide Receptor *Journal of Cell Biology*, 133(2).
- Teraoka, F., M. Hara, M. Nakagawa, and T. Sohmura. "Fabrication of Sintered Porous Poly(L-Lactide) Scaffold with Controlled Pore Size and Porosity." *Journal of Applied Polymer Science* 117, no. 3 (2010): NA-NA.
- Tsuchiya, K., Chen, G., Ushida, T., Matsuno, T., & Tateishi, T. (2004). The Effect of Coculture of Chondrocytes with Mesenchymal Stem Cells on their Cartilaginous Phenotype in vitro. *Materials Science and Engineering*.
- Varshney, R., Zhou, R., Hao, J., Yeo, S. S., Chooi, W. H., Fan, J., & Wang, D.-a. (2010). Chondrogenesis of Synovium-Derived Mesenchymal Stem Cells in Gene-Transferred Co-Culture System *Biomaterials*, 31.
- Verdonk, P., Forsyth, R., Wang, J., Almgvist, K., Verdonk, R., Veys, E., & Verbruggen, G. (2005). Characterisation of human knee meniscus cell phenotype. *Osteoarthritis Cartilage*, 548-560.
- Yoshikawa, K., Kitamura, N., Kurokawa, T., Gong, J. P., Nohara, Y., & Yasuda, K. (2013). Hyaluronic Acid Affects the in Vitro Induction Effects of Synthetic PAMPS and PDMAAm Hydrogels on Chondrogenic Differentiation of Atdc5 Cells, Depending on the Level of Concentration. *Musculoskeletal Disorders*, 14.
- Zhang, Z., McCaffery, M., Spencer, R., & Francomano, C. (2004). Hyaline cartilage engineered by chondrocytes in pellet culture: histological, immunohistochemical and

ultrastructural analysis in comparison with cartilage
explants. *Anatomical Society of Great Britain and Ireland*(205), 229-237.

Appendices:

Appendix A: Cell Passaging

- 1.) Aspirate media and wash cells two times with DPBS(-).
- 2.) Trypsinize cells for 10 minutes to digest the extracellular matrix and lift them off the plate.
- 3.) Add fresh media to stop the trypsin.
- 4.) Aspirate cell suspension and centrifuge for 5-10 minutes.
- 5.) Resuspend pelleted cells in fresh media and count or split as desired.
- 6.) Pipette desired amount of cells onto new plate filled with media and transfer to the incubator.

Appendix B: Alcian blue staining protocol

- 1.) Wash sample in 3% acetic acid, 10 minutes for each rinse.
- 2.) Incubate sample with Alcian blue stain for 15 minutes at 37° C, or 30 minutes at room temperature.
- 3.) Wash sample in 3% acetic acid, 10 minutes for each rinse.
- 4.) Wash sample in sterile water, 10 minutes for each rinse.
- 5.) Store stained samples in sterile water.

Appendix C: Scaffold seeding protocol

- 1.) Soak printed scaffolds and seeding wells in 70% isopropyl alcohol for a minimum of 2 hours.
- 2.) Use sterile forceps to remove scaffolds and seeding wells from isopropyl alcohol and place in a sterile tissue culture plate in the biosafety hood. Keep plates uncovered with the UV light on to allow the isopropyl alcohol to evaporate and complete the sterilization process.
- 3.) Use sterile forceps to place the scaffolds into their respective seeding wells, either the single or modular wells.

- 4.) Store PureCol EZ Gel in ice under the hood.
- 5.) Trypsinize cells, count, and perform serial dilutions until the desired cell concentration is reached.
- 6.) Pipette desired number of cells in less than 200 μ l of media into PureCol EZ Gel and mix thoroughly.
- 7.) Store PureCol EZ Gel at 25° C for 30 minutes.
- 8.) Pipette 245 μ l of cell hydrogel solution onto the single scaffolds and 650 μ l onto the modular scaffolds.
- 9.) Cover tissue culture plate and move to incubator for 90 minutes.
- 10.) Move tissue culture plate back to biosafety hood and remove scaffolds from seeding wells using sterile forceps. Care needs to be taken when removing the modular scaffolds without separating the two scaffold halves.
- 11.) Cover scaffolds with respective media and culture using standard methods.

Appendix D: Modular Scaffold Separation

- 1.) Using sterile forceps and a tissue culture plate, place modular scaffolds on their side and grip one of the scaffold halves with the sterile forceps.
- 2.) Using a sterile scalpel, carefully cut through the hydrogel connecting the two scaffold halves. Attempt using one clean cut to have a smooth surface on the inner face of the individual scaffold halves.
- 3.) While this cut is being performed carefully observe and keep track of which side of the scaffold halves is the inner face. Once separated place the inner face down onto the tissue culture plastic.
- 4.) Inner cells at a depth of 3mm can now be observed and stained for analysis.

Appendix E: Histological Tissue Processing and Microtome Sectioning

- 1.) Put scaffold in a processing cassette and store in Isopropyl Alcohol. If scaffold is modular, cut it into two pieces by following steps 1-2 of **Appendix D**.
- 2.) Process the Cassettes using a Tissue Processor under standard tissue processing conditions.
- 3.) Embed processed scaffolds in a paraffin wax.
- 4.) Use a Microtome to slice away wax until the surface of the scaffold is exposed.
- 5.) Soak the wax-embedded scaffold in acetone for 2-3 minutes to soften the PLA enough that 5-6 um slices can be cut using the microtome.
- 6.) Prior to sectioning the scaffold with the microtome, prepare several positively-charged test slides by labeling them and spreading a thin layer of Loctite(R) GO2 glue over the slide surface.
- 7.) Use the Microtome to generate 5-6 um sections from the acetone soaked scaffold. Carefully place sections directly on the glue-covered slide after cutting them (do not float samples on water as is typical for histology).
- 8.) Repeats steps 5-7 as necessary when the scaffold becomes too difficult to section or until sections of the desired scaffold depth have been generated.

Appendix F: Hematoxylin and Eosin Staining Protocol

This process was adapted from the Gateway Park Core Labs procedure provided by Hans B. Snyder. Each step is done in a separate reagent bath.

- 1.) De-paraffinize slides in xylene (1) for 2 minutes (re-use)
- 2.) De-paraffinize slides in xylene (2) for 2 minutes (re-use)
- 3.) Clear slides in 100% ethanol for 2 minutes
- 4.) Clear slides in 100% ethanol for 2 minutes
- 5.) Hydrate slides in 95% ethanol for 2 minutes
- 6.) Hydrate slides in running DI water for 5 minutes

- 7.) Stain slides in Harris Hematoxylin for 5 minutes (re-use)
- 8.) Wash slides in running DI water for 5 minutes
- 9.) Stain in Eosin for 1 minute (re-use)
- 10.) Dehydrate in 95% ethanol for 1 minute
- 11.) Dehydrate in 100% ethanol for 1 minute
- 12.) Dehydrate in 100% ethanol for 1 minute
- 13.) Dehydrate in 100% ethanol for 5 minute
- 14.) Clear in xylene (4) for 2 minutes (re-use).
- 15.) Clear in xylene (5) for 1-5 minutes (re-use). During this step, observe the test slides. If the glue on the slide begins to bubble/deform, immediately remove slides from xylene and seal using a coverslip and copious slide glue. Otherwise, coverslip the slides after the xylene wash is finished.
- 16.) Wait for the glue to dry and image using a light microscope.

Solutions:

Stock Eosin Solution: 1.0g Eosin Y, 100.0mL DI H₂O

Stock Phloxine: 1.0g Phloxine B, 100.0mL DI H₂O

Working Eosin Solution: 100.0mL Stock Eosin, 10.0mL Stock Phloxine, 280.0mL 95% Ethanol, 4.0mL Glacial Acetic Acid

Harris Hematoxylin Solution: Store bought; filter before each use.

Appendix G: Cell Folding Images

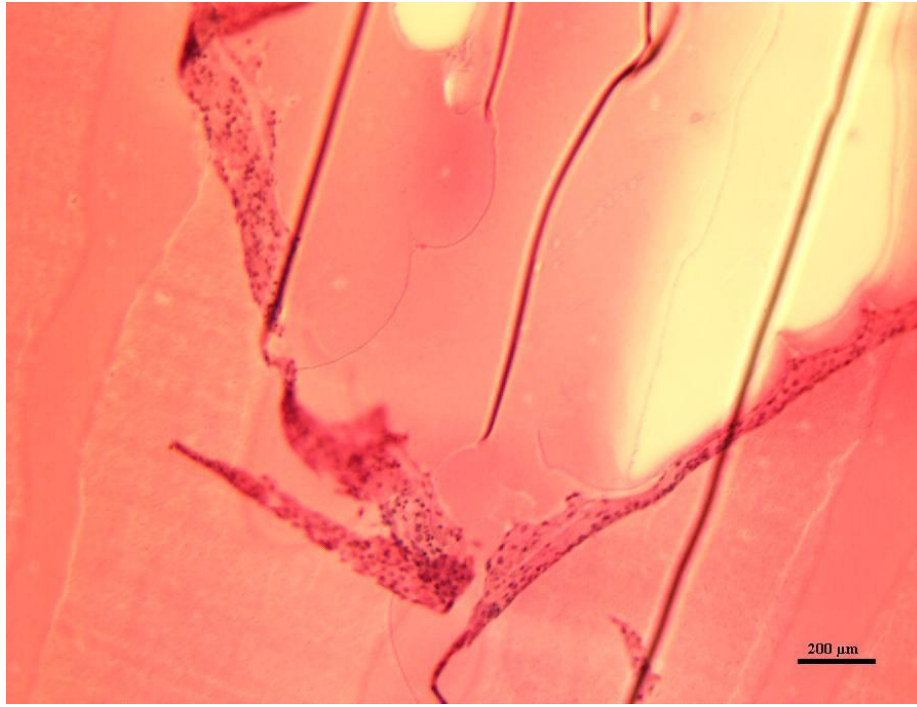


Figure H.1: 10x image of cell folding from an H&E stained Original Protocol Outer Scaffold Slice